AD-A120 649 A STUDY OF THE DEFECTS PRODUCED BY THE GROWTH POST TREATMENT AND FABRICAT..(U) OKLAHOMA STATE UNIV STILLWATER DEPT OF PHYSICS L E HALLIBURTON ET AL. 1/1

UNCLASSIFIED AUG 82 RADC-TR-82-213 F19628-80-C-0086 F/G 20/6 NL

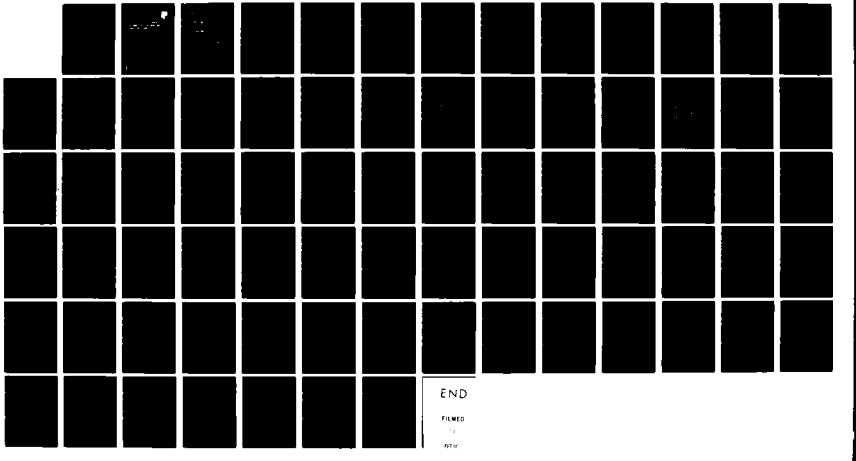

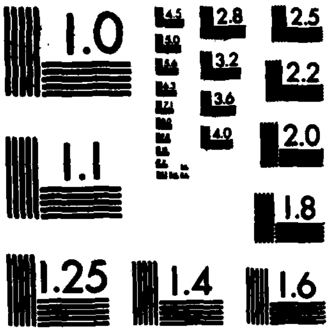

MICROCOPY RESOLUTION TEST CHART
NATIONAL BUREAU OF STANDARDS-1963-A

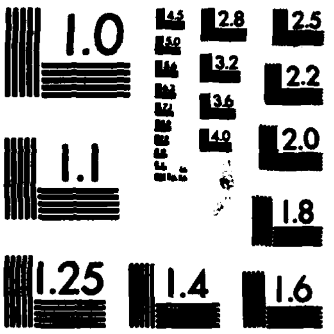

MICROCOPY RESOLUTION TEST CHART
NATIONAL BUREAU OF STANDARDS-1963-A

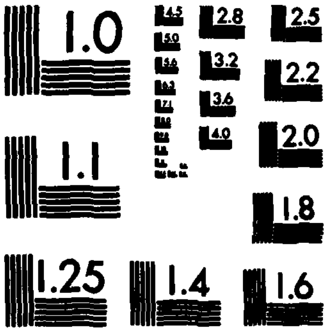

MICROCOPY RESOLUTION TEST CHART
NATIONAL BUREAU OF STANDARDS-1963-A

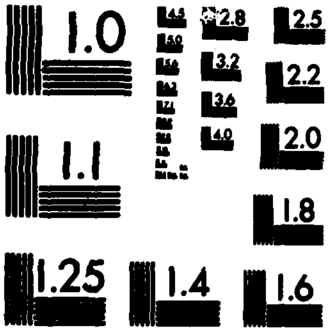

MICROCOPY RESOLUTION TEST CHART
NATIONAL BUREAU OF STANDARDS-1963-A

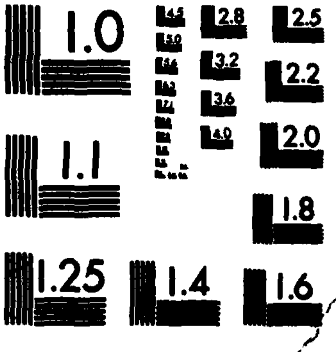

MICROCOPY RESOLUTION TEST CHART
NATIONAL BUREAU OF STANDARDS-1963-A

RADC-TR-82-213
Interim Report
August 1982

AD A120649

A STUDY OF THE DEFECTS PRODUCED BY THE GROWTH, POST TREATMENT, AND FABRICATION OF QUARTZ DEVICES

Oklahoma State University

Larry E. Halliburton
Joel J. Martin
William A. Sibley

APPROVED FOR PUBLIC RELEASE; DISTRIBUTION UNLIMITED

DTIC
ELECTE
A

ROME AIR DEVELOPMENT CENTER
Air Force Systems Command
Griffiss Air Force Base, NY 13441

82 10 25 051

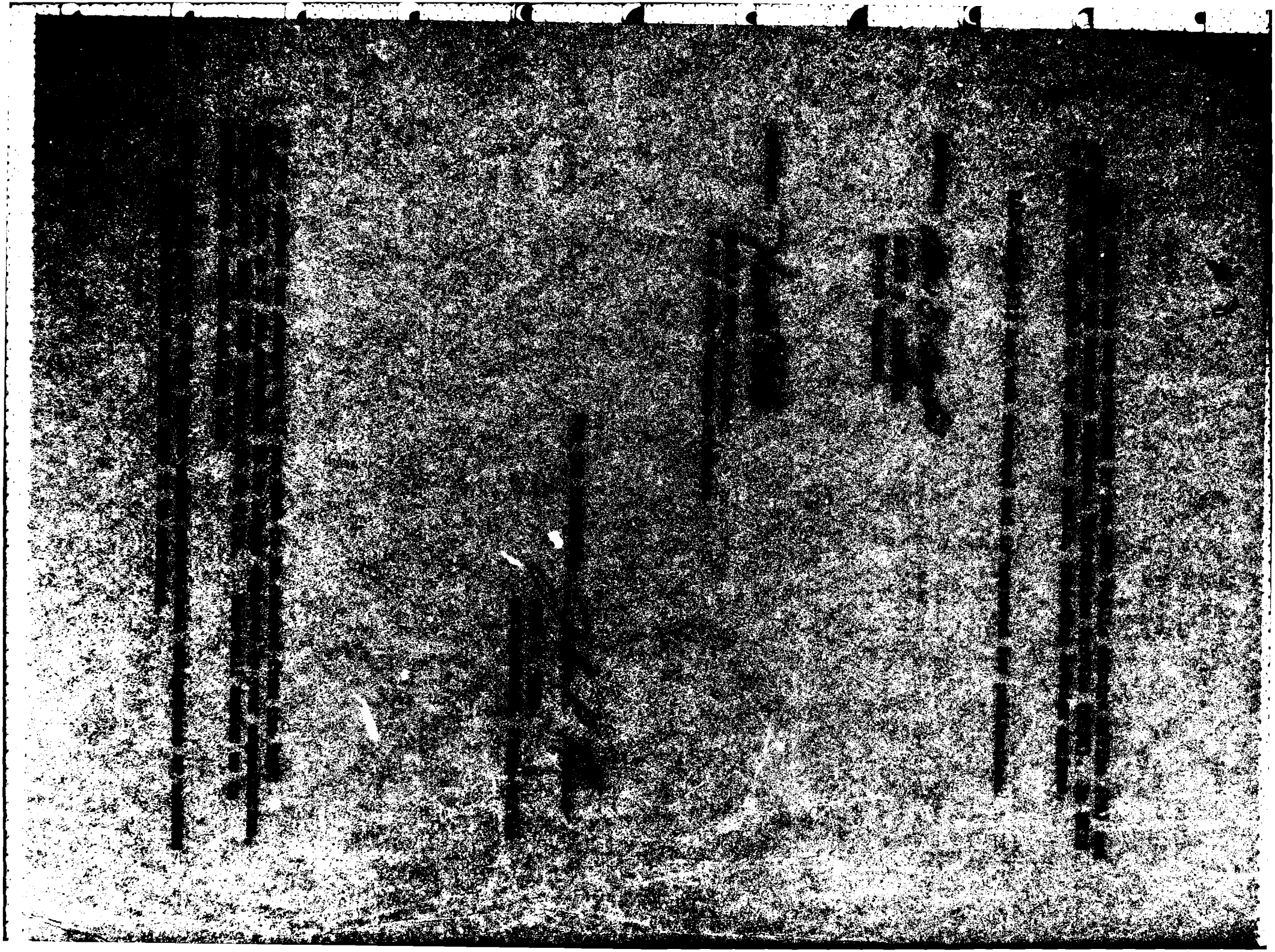

UNCLASSIFIED

SECURITY CLASSIFICATION OF THIS PAGE (When Data Entered)

REPORT DOCUMENTATION PAGE		READ INSTRUCTIONS BEFORE COMPLETING FORM
1. REPORT NUMBER RADC-TR-82-213	2. GOVT ACCESSION NO. AD-A120 649	3. RECIPIENT'S CATALOG NUMBER
4. TITLE (and Subtitle) A STUDY OF THE DEFECTS PRODUCED BY THE GROWTH, POST TREATMENT AND FABRICATION OF QUARTZ DEVICES		5. TYPE OF REPORT & PERIOD COVERED Interim Report April 81 - March 82
		6. PERFORMING ORG. REPORT NUMBER N/A
7. AUTHOR(s) Larry E. Halliburton Joel J. Martin William A. Sibley		8. CONTRACT OR GRANT NUMBER(s) F19628-80-C-0086
9. PERFORMING ORGANIZATION NAME AND ADDRESS Oklahoma State University Department of Physics Stillwater OK 74078		10. PROGRAM ELEMENT, PROJECT, TASK AREA & WORK UNIT NUMBERS 61101F 2306J135
11. CONTROLLING OFFICE NAME AND ADDRESS Rome Air Development Center (ESM) Hanscom AFB MA 01731		12. REPORT DATE August 1982
		13. NUMBER OF PAGES 76
14. MONITORING AGENCY NAME & ADDRESS(if different from Controlling Office) Same		15. SECURITY CLASS. (of this report) UNCLASSIFIED
		15a. DECLASSIFICATION/DOWNGRADING SCHEDULE N/A

16. DISTRIBUTION STATEMENT (of this Report)

Approved for public release; distribution unlimited.

17. DISTRIBUTION STATEMENT (of the abstract entered in Block 20, if different from Report)

Same

18. SUPPLEMENTARY NOTES

RADC Project Engineer: Alton F. Armington (ESM)

19. KEY WORDS (Continue on reverse side if necessary and identify by block number)

Quartz	Aluminum	Vacancies
Acoustic Loss	Alkali Intersitials	X-Ray
EPR	IR Absorption	Luminescence
Electrodiffusion	Sweeping	

20. ABSTRACT (Continue on reverse side if necessary and identify by block number)

At Oklahoma State University we are using acoustic loss, IR, ESR, and current-versus-time measurements to characterize the electrodiffusion process in quartz. Commercial sweeping is done in air and replaces the alkali ions with protons. We are carrying out this study using H_2, D_2, and vacuum atmospheres. The current-versus-time curves for H_2 and D_2 electrodiffusion show a rapid initial drop and then level off to a small steady current. We believe that the initial drop is caused by the rapid removal

DD FORM 1 JAN 73 1473 EDITION OF 1 NOV 65 IS OBSOLETE

UNCLASSIFIED

SECURITY CLASSIFICATION OF THIS PAGE (When Data Entered)

of the alkali ions. For alkali sweeps, steady currents are observed and only small electric fields are required. Acoustic loss measurements verify that Na^+ and Li^+ can be readily interchanged. The results for K^+ are, at this time, uncertain. An initial vacuum electrolysis run showed that the current stopped after a short time, and subsequent IR and ESR tests showed that only a small amount of hydrogen was swept into the sample. We believe that the electrodiffusion can continue only as long as replacement ions (in this case protons) are brought into the sample. A study of the acoustic loss spectrum of a series of 5 MHz 5th overtone AT-cut resonator blanks all fabricated from the same bar of Premium Q grade quartz as a function of electrolysis and irradiation is nearly complete. Na-swept samples show a very large 54 K loss peak. This shows that in as-grown quartz most of the Al sites are compensated by Li^+. No loss peaks were observed at temperatures less than 100°C which could be attributed to the Al-Li^+ or Al-OH centers. Irradiation at room temperature removed the Na loss peak and produced peaks at 25 K, 100 K, and 135 K. An isochronal anneal study shows that these three peaks are caused by the Al-hole center. The work on K-swept material is not yet complete.

The x-ray induced "blue" emission from commercially available, high-quality synthetic quartz has been studied between 80 and 300 K. Three overlapping bands, each having a different quenching temperature, have been experimentally resolved in the as-grown crystals. These bands peak at 440 nm, 425 nm, and 380 nm; their half-widths are 0.64 eV, 0.75 eV, and 0.92 eV; and they thermally quench in the 120-160 K, 170-210 K, and 220-270 K regions, respectively. An intense electron irradiation at room temperature or an electrodiffusion (sweep) in a hydrogen atmosphere eliminates the band at 380 nm. Our results suggest that the 380 nm band arises from recombination of an electron with a hole trapped adjacent to an alkali-compensated aluminum (i.e., and Al-M^+ center). The origins of the bands at 440 nm and 425 nm remain unknown. As an application of these results, a screening test is described which would maintain quality control during selection of quartz bars for use in precision frequency control devices.

Electron spin resonance has been used to study three similar, but distinct, S = 1 defects (labeled E" centers) in high-quality synthetic quartz crystals. These centers are produced by electron irradiation and their concentrations depend on the irradiation temperature, the nature of previous irradiations and thermal anneals, and whether the sample is swept or unswept. the radiation-induced mobility of interstitial alkali ions (Li^+ and Na^+) correlates with the production of E" centers.

A series of RADC-grown quartz stones have been run through our ESR test for aluminum content. Pure Z-growth samples from several stones showed less than 1 ppm aluminum. The OH bands at 3585, 3437, and 3400 cm^{-1} which are present in as-grown quartz have been measured as a function of the growth rate for stones grown at RADC. The 3367 cm^{-1} Al-OH has also been measured for these samples after a room temperature irradiation. All of these OH-related defects increase markedly for stones grown at rates faster than 0.7mm/day.

TABLE OF CONTENTS

Accession For
DTIC COPY INSPECTED

I. INTRODUCTION AND SUMMARY

The defect structures in crystalline SiO_2, better known as quartz, and in related materials continue to be of considerable interest. Alpha-quartz, which is piezoelectric, finds application in a variety of electronic devices (e.g., high precision oscillators, filters, accelerometers, etc.) where sensitivity and stability are crucial operating criteria. However, a number of problems confront the systems designer when attempting to incorporate such precision frequency control devices into operational units. For example, in the case of quartz-controlled clocks, a major consideration is long term stability. Frequency shifts due to aging can disable an entire system. Equally important, quartz oscillators flown on satellites may experience low-level radiation which cause frequency shifts and alter the aging characteristics. The radiation response and, most likely, part of the aging of quartz crystals are related to the defects produced during crystal growth or during subsequent treatment.[1-5]

At Oklahoma State University we are using acoustic loss, IR, ESR, and current-versus-time measurements to characterize the electrodiffusion process in quartz. Commercial sweeping is done in air and replaces the alkali ions with protons. We are carrying out this study using H_2, D_2, and vacuum atmospheres. The current-versus-time curves for H_2 and D_2 electrodiffusion show a rapid initial drop and then level off to a small steady current. We believe that the initial drop is caused by the rapid removal of the alkali ions. For alkali sweeps, steady currents are observed and only small electric fields are required. Acoustic loss measurements verify that Na^+ and Li^+ can be readily interchanged. The results for K^+ are, at this time, uncertain. An initial vacuum electrolysis run showed that the current stopped after a short time, and subsequent IR and ESR tests showed that only a small amount of hydrogen was swept into the sample. We believe that the electrodiffusion can

continue only as long as replacement ions (in this case protons) are brought into the sample.

A study of the acoustic loss spectrum of a series of 5 MHz 5th overtone AT-cut resonator blanks all fabricated from the same bar of Premium Q grade quartz as a function of electrolysis and irradiation is nearly complete. Na-swept samples show a very large 54 K loss peak. This shows that in as-grown quartz most of the Al sites are compensated by Li^+. No loss peaks were observed at temperatures less than 100°C which could be attributed to the Al-Li^+ or Al-OH centers. Irradiation at room temperature removed the Na loss peak and produced peaks at 25 K, 100 K, and 135 K. An isochronal anneal study shows that these three peaks are caused by the Al-hole center. The work on K-swept material is not yet complete.

The x-ray-induced "blue" emission from commercially available, high-quality synthetic quartz has been studied between 80 and 300 K. Three overlapping bands, each having a different quenching temperature, have been experimentally resolved in the as-grown crystals. These bands peak at 440 nm, 425 nm, and 380 nm; their half-widths are 0.64 eV, 0.75 eV, and 0.92 eV; and they thermally quench in the 120-160 K, 170-210 K, and 220-270 K regions, respectively. An intense electron irradiation at room temperature or an electrodiffusion (sweep) in a hydrogen atmosphere eliminates the band at 380 nm. Our results suggest that the 380 nm band arises from recombination of an electron with a hole trapped adjacent to an alkali-compensated aluminum ion (i.e., an Al-M^+ center). The origins of the bands at 440 nm and 425 nm remain unknown. As an application of these results, a screening test is described which would maintain quality control during selection of quartz bars for use in precision frequency control devices.

Electron spin resonance has been used to study three similar, but distinct, S = 1 defects (labeled E" centers) in high-quality synthetic quartz

crystals. These centers are produced by electron irradiation and their concentrations depend on the irradiation temperature, the nature of previous irradiations and thermal anneals, and whether the sample is swept or unswept. The radiation-induced mobility of interstitial alkali ions (Li^+ and Na^+) correlates with the production of E'' centers.

A series of RADC-grown quartz stones have been run through our ESR test for aluminum content. Pure Z-growth samples from several stones showed less than 1 ppm aluminum. The OH bands at 3585, 3437, and 3400 cm^{-1} which are present in as-grown quartz have been measured as a function of the growth rate for stones grown at RADC. The 3367 cm^{-1} Al-OH^- has also been measured for these samples after a room temperature irradiation. All of these OH-related defects increase markedly for stones grown at rates faster than 0.7mm/day.

II. ELECTRODIFFUSION

A. Introduction

Interstitial alkali ions and protons are trapped by substitutional aluminum ions[5] and, quite possibly, by other defects in alpha-quartz. These interstitials lie in the large c-axis channels and they can diffuse along the channels when thermally liberated from their traps. This thermal diffusion must be at least partly responsible for the annealing behavior of radiation induced defects.[6,7,8] A technologically important result occurs when an electric field applied parallel to the c axis is used to force these interstitial ions out of the sample and replace them with others. King,[9] making use of this characteristic, was among the first to develop the electrodiffusion (sweeping) process as a method for changing the concentration of specific interstitial cations (i.e., H^+, Li^+, Na^+, etc.) within a given quartz crystal. The process was later used by Katz[10] to "sweep" hydrogen and alkali ions into and out of quartz. Fraser[11] described the basic technology

for the selective sweeping of alkalis and Kreft[12] has shown that holes can be swept into quartz if the process is carried out in vacuum at temperatures above the phase transition. Brown, O'Conner, and Armington[13] have investigated alkali sweeping and the use of an inert gas atmosphere. A number of studies have shown that the radiation hardness of oscillators is significantly enhanced if electrodiffusion is used to replace the alkalis in quartz with protons.[2,14,15] Recently, Jain and Nowick[16] have investigated ionic conductivity in both synthetic and natural quartz.

A systematic study of the electrolysis process in quartz is presently underway. The interstitial alkali ions, which act as charge compensators for the substitutional Al^{3+} ions in as-grown quartz, are thermally released from the aluminim traps at high temperature and then drift along the relatively large c-axis channels. If an electric field is applied parallel to the c axis and if a source of replacement ions is present, the alkali ions originally in the crystal can be removed. Conventional commercial sweeping is done in air and the replacement ions are protons, apparently originating in the water vapor contained in the surrounding air. On the other hand, if a salt such as NaCl is first deposited at the positive electrode then the sample can be doped with that particular alkali.

B. Experimental Procedure

The present sweeping system at Oklahoma State University consists of a vitreous silica jacket evacuated with a diffusion pump. The jacket is heated by an external clamshell furnace. This system allows us to electrolyze quartz either in a controlled atmosphere or in a vacuum on the order of 2×10^{-6} to 5×10^{-6} Torr. The sample is usually mounted between graphite clamps. We have also assembled a copper-gasketed turbomolecular-pumped system with an internal heater for sweeping studies at pressures on the order of 10^{-8} Torr. Work with this latter system has been delayed because of a pump malfunction.

Our present sweeping procedure begins by vapor depositing gold electrodes on the two sample faces, which is a Z plate in the case of optical and ESR experiments or is a plano-convex AT-cut resonator blank in the case of acoustic loss studies. Then the electrolysis is carried out in the desired atmosphere at a temperature between 485 and 490°C. During sweeping, the current through the sample is recorded as a function of time. In order to sweep Li, Na, or K into a crystal, the appropriate salt is vapor deposited first and then the gold electrodes are deposited. The graphite clamps are baked-out under vacuum before the alkali or vacuum electrolysis is performed. All such alkali sweeping is done in a vacuum of 5×10^{-6} Torr or better. Electric fields of 15 to 30 volts/cm readily sweep the alkali ions into a sample, whereas much higher fields of approximately 1000 to 3000 volts/cm are used in the hydrogen and vacuum electrolysis.

C. Results and Discussion

Figure 1 shows the current-versus-time curves obtained by sweeping with Na, H_2, and in vacuum. Similar curves were found for Li, K, and D_2. The samples used in this study were Z-plate optical samples and were all cut from Electronic Grade bar EG-B. The alkali sweeps were terminated after approximately 30 minutes to prevent depletion of the salt-source film at the positive electrode, while the H_2, D_2, and vacuum sweeps were run for 16 to 20 hours. In the case of the vacuum sweep, the current went essentially to zero after about 20 minutes, which indicates that the electrolysis stopped at that point. Following the sweeps, infrared absorption spectra were run on all of the samples. Table 1 compares the height of the 3367 cm^{-1} band (due to $Al\text{-}OH^-$ centers) for the different runs.

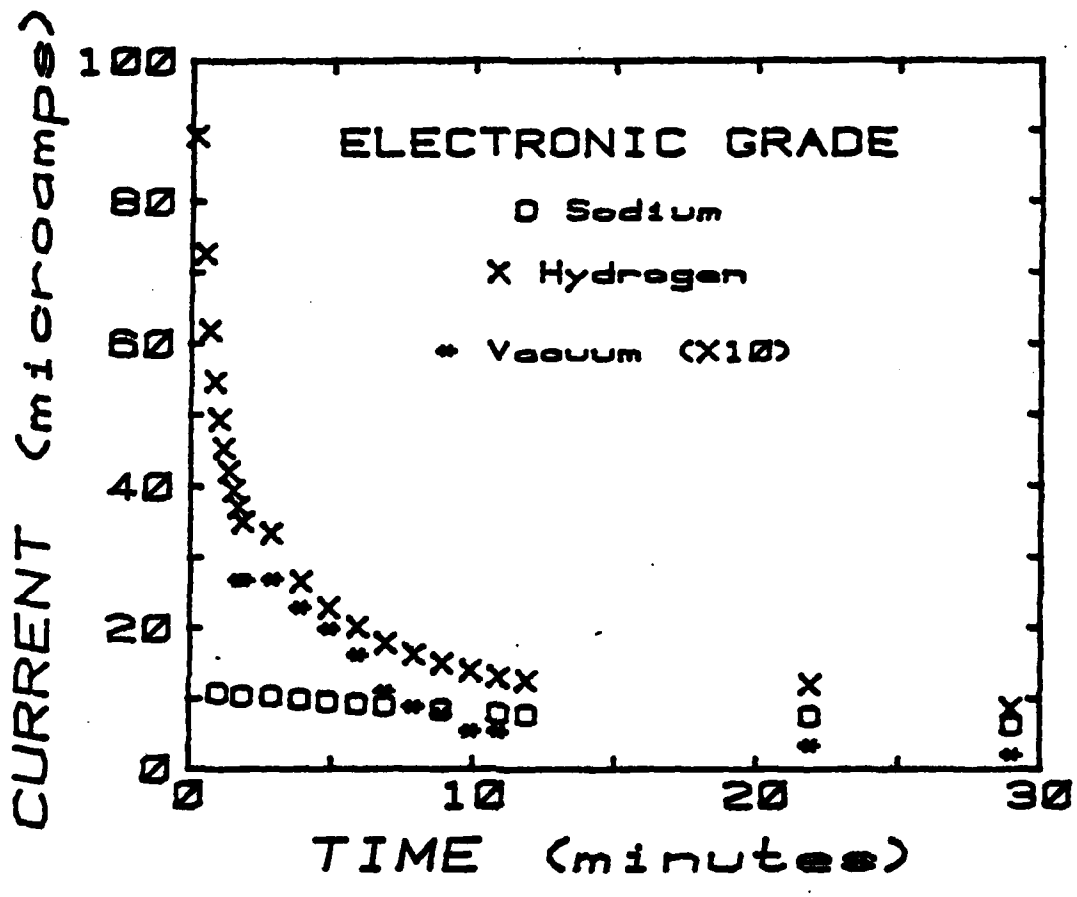

Figure 1. Current-versus-time results from a variety of sweeping experiments

Table I. Absorption coefficient of the Aℓ-OH^- infrared band at 3367 cm^{-1} in EG-B electronic grade samples after various types of electrolysis.

Sweep	$\alpha(cm^{-})$
as-received	~0
H_2	1.10
D_2	1.27 (at 2494 cm^{-1})
Li	~0
Na	0.045
K	~0
vacuum	0.35

The H_2 and D_2 sweep current-versus-time curves show a rapid initial drop and then leveling off to a final steady current of a few microamperes. We believe that the initial drop is caused by the rapid removal of the highly mobile alkali ions and that the steady final current represents the drift of protons (or deuterons) through the sample. No significant changes were observed in the 3585 cm^{-1}, 3437 cm^{-1}, and 3400 cm^{-1} infrared absorption bands in any of the sweep runs, except in the case of deuterium. When a D_2 atmosphere was used, these bands were completely replaced by their OD^-analogs.[13] The Aℓ-OH^-bands at 3367 cm^{-1} and 3306 cm^{-1} were, of course, produced by the H_2 sweep, as were their OD^-analogs when a D_2 atmosphere was used.

The alkali sweeps of the EG-B samples gave steady current densities in the 2-4 $\mu A/cm^2$ range for electric fields of 15 V/cm. Comparable steady final current densities for H electrolysis required electric fields of 3000 V/cm. Thus, the alkali ions appear to be approximately 200 times more mobile than protons. The results described in the acoustic loss section of this report on Li^+ and Na^+ swept resonators show that we have successfully swept both ions into quartz. The very large Al-Na^+ loss peak that is produced by Na^+ sweeping indicates that in as-grown Premium Q grade material Li^+ is the dominant alkali.

At this time the K sweep results must be considered preliminary. The current-versus-time and the current magnitudes during the sweep were typical of our other alkali results. The Q^{-1} spectrum of a K-swept Premium Q grade blank showed a fairly large 55 K loss peak, $\Delta Q^{-1} = 2 \times 10^{-5}$, which indicates that approximately 10% of the aluminum ions were converted to Al-Na^+ centers by the sweep. Although Na contamination of the K salt cannot be ruled out, the basic process was the same as used in the previous Li sweep which did not produce any Na peaks. The question is: Did the sweep result in a transfer of Na from other sites in the sample to the aluminum site with, of course, the K going into the initial Na sites?

The data obtained from the vacuum-swept sample are quite interesting. The Al-OH^- center infrared absorption band for this sample is only 30% as high as the equivalent band in the H_2-swept sample. Thus, the vacuum-swept sample appears to be only partially swept. This result was verified when ESR samples were cut from the larger optical samples and then subjected to our ESR sweeping evaluation test. Results from the ESR test showed that the vacuum-swept sample was actually only 25% swept and the H_2-swept sample was 95% swept. We interpret the partial sweep in vacuum as follows. The

electrolysis can continue only as long as replacement ions (in this case protons) are brought into the crystal. When no more replacement ions are available, an internal space charge field develops which opposes the external applied electric field. The actual electric field at the interstitial ion sites becomes zero and no further preferential diffusion occurs. The source of the protons initially brought into the sample during our vacuum sweep is unknown; however, hydrogen is a prevasive contaminent in vacuum systems. To minimize this source of protons, the graphite holder and sweeping system had been baked out over night at 500°C. In order to clarify and understand the results just described, additional studies must be done on vacuum sweeping.

D. Summary

We have shown that Li^+ and Na^+ ions as well as protons can be efficiently swept into quartz. Hydrogen (or air) sweeping effectively replaces the alkalis at the aluminum. The kinetics of the alkali and proton motion during electrolysis are not yet understood. It also appears that additional unidentified alkali traps are present. Our results indicate that electrolysis in a good vacuum with no alkali salt source film stops well before all of the alkalis are removed because there is nothing to bring in as replacement ions.

III. ALUMINUM-RELATED ACOUSTIC LOSS IN AT-CUT QUARTZ CRYSTALS

A. Introduction

Alpha-quartz is used in a wide vaiety of precision electronic devices where aging and radiation-induced instabilities are undesirable. It is now well-known that quartz-controlled oscillators may exhibit transient and steady-state frequency and Q shifts when exposed to ionizing radiation.[4,17-19] Early results obtained by King[9] and other investigators[2,3,5,24] suggested that these effects were associated with the presence of impurities.

Substitutional Al^{3+} is present in all quartz and requires charge compensation. Examples of such charge compensators are interstitial Li^+ or Na^+ ions, or holes or protons at an oxygen ion adjacent to the aluminum. The proton forms an OH^- molecule which is infrared active.[5,10] The Al-Na^+ defect is responsible for the acoustic loss peak observed near 50 K in 5 MHz 5th overtone AT-cut crystals.[11] Irradiation at room temperature destroys the Al-Na^+ centers,[8,9] and this is responsible for much of the steady state frequency offset. Recent work at Oklahoma State University has shown that the alkali ions become mobile under irradiation only if the temperature is greater than 200 K.[6,7,8] Following a room temperature irradiation, either a hole which can be observed by ESR techniques or a proton is found trapped on an oxygen adjacent to the Al^{3+}. The interstitial alkali ions are usually in the relatively large c-axis channels and at high temperatures can move along the channel under an applied electric field. King,[9] and later Kats[10] and Fraser,[11] used this technique to "sweep" hydrogen and specific alkalis into the sample. Sweeping hydrogen in to replace the alkalis has been shown to improve the radiation hardness of quartz oscillators.[3]

The identification of both growth and radiation-induced defects which affect the performance of quartz resonators is an important part of our project. Recently, using sweeping, IR absorption, and acoustic loss measurements, Martin and Doherty[20] reported that the Al-OH^- center does not have an acoustic loss peak at temperatures below 370 K. They also reported that irradiation of both unswept and H_2-swept Premium Q quartz resonator blanks produced acoustic loss peaks at 25 K and 100 K and a broad loss peak between 125 K and 165 K. King and Sander[4] had earlier reported the two higher temperature peaks and had suggested that they were caused by the Al-hole center. The 25 K peak had also been observed earlier and was attributed to

changes in the interaction between the resonant vibration of the blank and the thermal phonons.[1] We report here a comparison of the acoustic loss spectra of as-received, Li^+, Na^+, and H^+ swept resonators fabricated from the same bar of Premium Q grade quartz. We also report an isochronal anneal study of the three loss peaks induced by a room temperature irradiation which shows that they are associated with the Aℓ-hole center.

B. Experimental Procedure

All samples for this study were cut from an unswept pure Z growth Sawyer Premium Q bar of cultured quartz that has been given an in-house designation PQ-E. Samples from this bar have been extensively studied at Oklahoma State University using ESR,[5,7] IR, and acoustic loss techniques. All of these investigations show that the bar is of high quality but that it contains somewhat more aluminum (10-15 ppm) than the average Premium Q material (5-8 ppm). Consequently, aluminum-related effects are more readily observed.

Five MHz 5th overtone AT-cut plano convex resonator blanks of the Warner design were fabricated for this study by K&W Mfg., Prague, OK. The acoustic loss, Q^{-1}, of the resonator blanks was measured by the log decrement method from 5 to 300 K. The measurements were made in a variable temperature helium Dewar with the blanks mounted in a gap holder similar to the one described by Fraser.[1] The blank was driven for 10 ms at its series resonant frequency and then allowed to freely decay. The decaying rf signal was detected with a superheterodyne detector and displayed on a variable persistence storage oscilloscope. The exponential decay times were measured using a window detector to gate a digital timer.

Electrolysis, or sweeping, was carried out at temperatures of 470-480°C in a controlled atmosphere system. This system allowed the use of H_2, D_2, or gettered-N_2 atmospheres, or an oil-diffusion pumped vacuum of approximately

2×10^{-6} Torr. For the acoustic loss studies, the AT-cut resonator blanks were directly swept. Vapor-deposited Au electrodes were used. For the Li or Na sweeping runs, LiCl or NaCl was vapor deposited on the sample surface and then an Au electrode was deposited over the salt layer. The Li and Na sweeps were carried out in a vacuum better than 5×10^{-6} Torr. Infrared absorption scans show that Al-OH^- centers are present in the H_2-swept sample but not in the alkali swept samples.

Irradiations were carried out at room temperature using 1.7 MeV electrons from a Van de Graaff accelerator. Typical doses were approximately 2000 J/cm^3 ($\sim 10^8$ rads). This dose is not expected to produce significant knock-on damage, but it has been shown to saturate the Al-related defects. The production of Al-OH^- centers by the irradiation was measured by a liquid nitrogen temperature polarized infrared scan on the resonator blank.

C. Results and Discussion

Figure 2 compares the acoustic loss, Q^{-1}, spectra for unswept, Li-swept, and Na-swept PQ-E series resonator blanks. The unswept blank shows a small Al-Na^+ loss peak at 55 K with a height ΔQ^{-1} of approximately 0.5×10^{-6}. The Li sweep removed this peak and did not introduce any new peaks. The Na-swept blank showed a very large 55 K peak with $\Delta Q^{-1} = 2 \times 10^{-4}$ as shown in Figure 2. Since the material from which these blanks were fabricated contains 10 to 15 ppm aluminum, we conclude that the concentration, C, of Al-Na^+ centers is given by

$$C = [5\ (\pm\ 20\%) \times 10^4]\,\Delta Q^{-1}$$

where C is in ppm and ΔQ^{-1} is the height of the 55 K Al-Na^+ loss peak, thus, the unswept PQ-E blank probably contains about 0.3 ppm Al-Na^+ centers; the remaining 10 to 15 ppm of aluminum must be compensated by Li^+. Since the

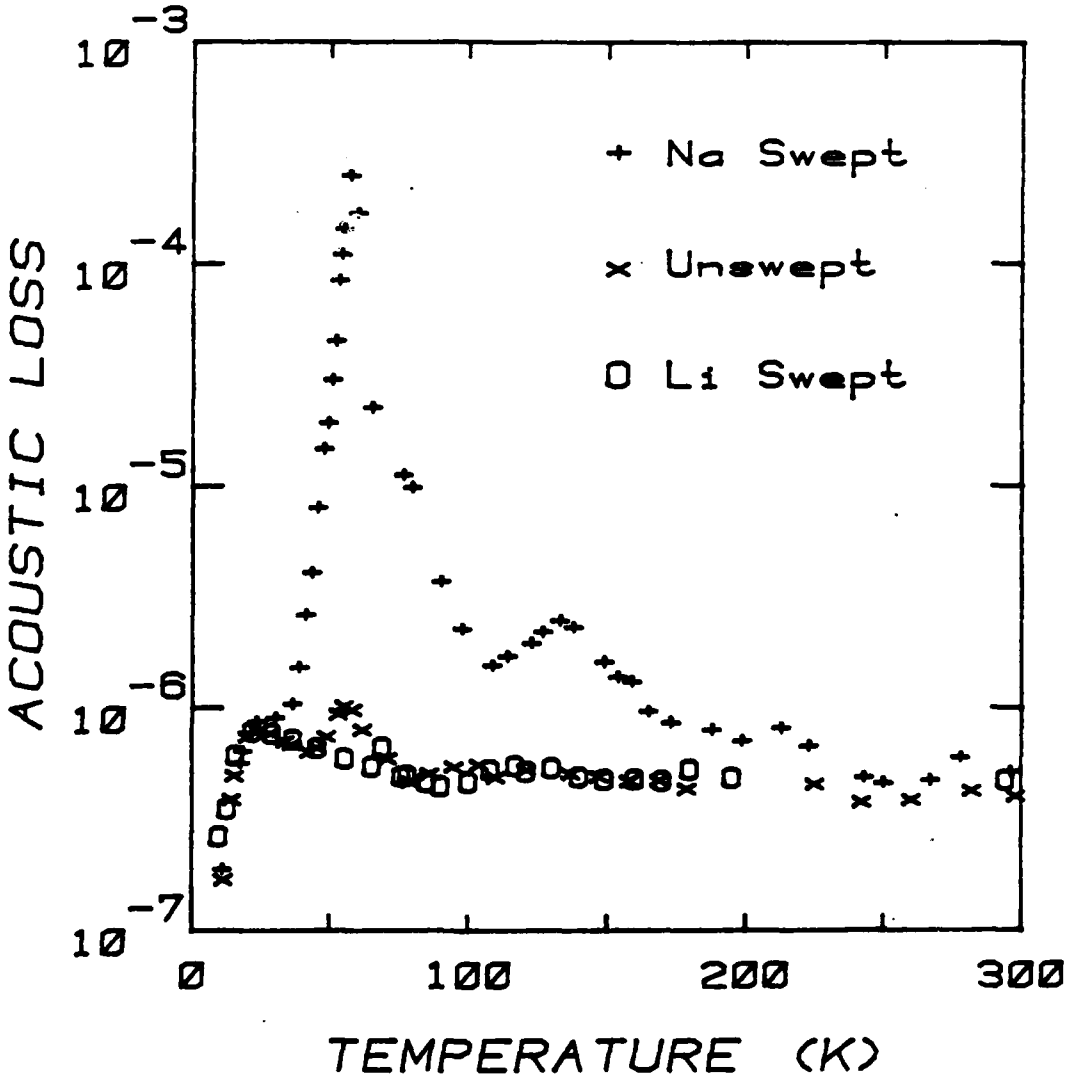

Figure 2. The acoustic loss spectra of unswept, Li swept and Na swept resonator blanks fabricated from a Premium Q bar that contains 10-15 ppm aluminum is shown.

mineralizer used in growing Premium Q quartz is predominantly $NaCO_3$, the essentially total exclusion of Na^+ from the aluminum sites by the addition of a small amount of $LiCO_3$ to the solution is remarkable.[22] Since both the unswept and Li-swept blanks must contain 10-15 ppm Al-Li^+ centers, we believe that the Al-Li^+ center does not couple to the AT-cut thickness-shear mode. An additional, much smaller, loss peak related to the Al-Na^+ center was observed at approximately 135 K in the Na-swept blank. Park and Nowick[23] have also observed two Na-related peaks in their dielectric loss measurements.

Figure 3 compares the acoustic loss spectra for the unswept, Li-swept, and H-swept blanks. The results for the Li and H-sweeps are essentially identical, as were the results for a D-sweep which were omitted from Fig. 3 for clarity. Infrared absorption measurements made at liquid nitrogen temperature show that the H-swept blank contains 10-15 ppm Al-OH^- centers. Thus, it appears that neither the Al-OH^- or the Al-OD^- centers show significant acoustical loss peaks at temperatures below about 370 K. It should be noted that at higher temperatures, the interstitial alkali ions become thermally liberated from the Al^{3+} trapping site and diffuse along the c-axis channels. This diffusion causes an acoustic loss which increases exponentially with temperature.[1] Lipson et al.[24] and Koehler[25] have shown that this high temperature loss is not present in H-swept quartz which contains no alkali ions, and therefore, must be caused by the alkali diffusion.

Recently, Martin and Doherty[20] reported that irradiation of unswept and H_2-swept PQ-E resonator blanks at room temperature produced loss peaks at 25 K and 100 K and a broad loss between 125 and 165 K. The peaks were much larger in the unswept material than in the H_2-swept blank. The room temperature irradiation also removed the Al-Na^+ loss peak which was present initially in

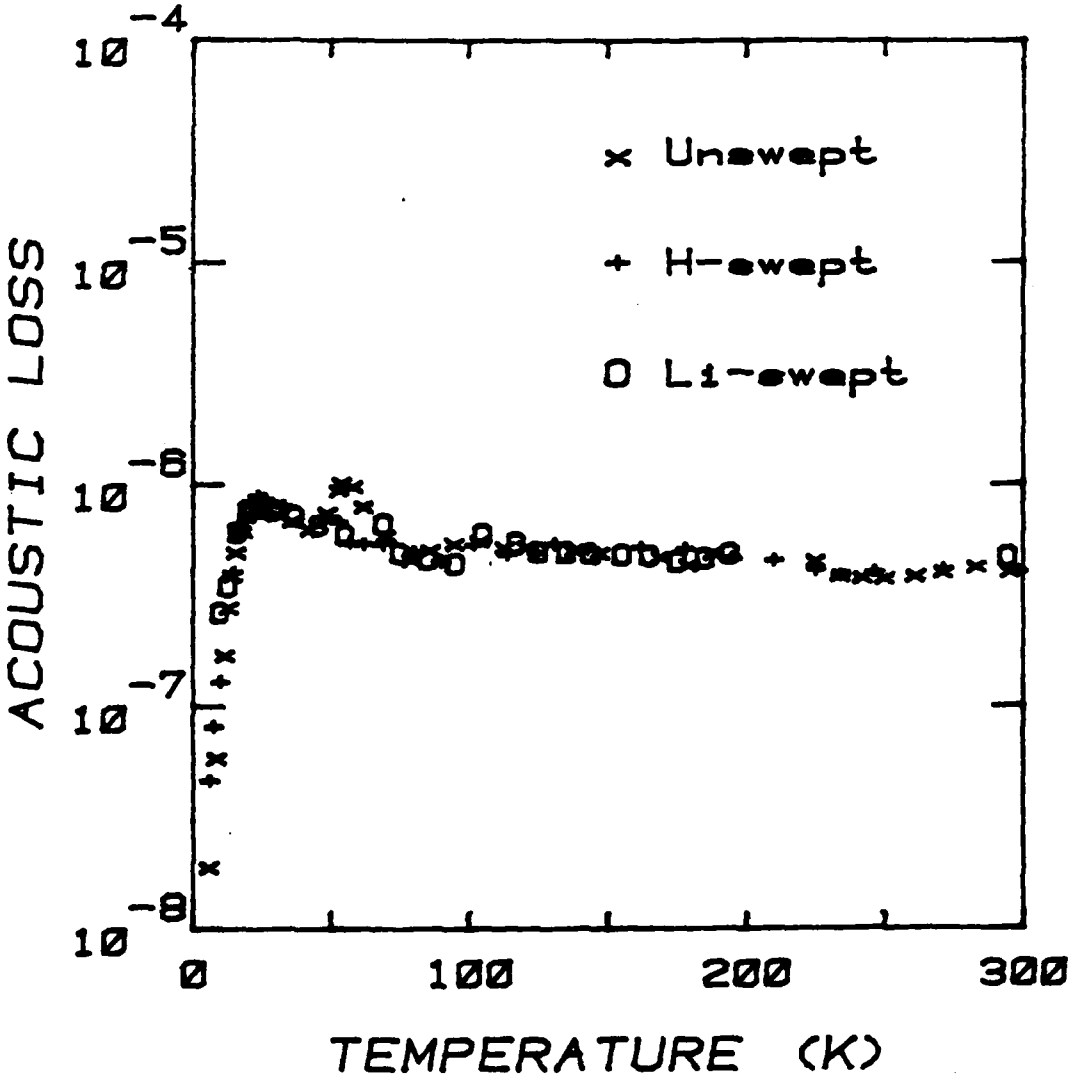

Figure 3. The acoustic loss spectra of unswept, Li swept and H swept resonator blanks is shown.

the unswept blank. King and Sander[4] have previously observed the peak at 100 K and the broad loss between 125 K and 165 K. They attributed these loss peaks to the Al-hole center. Martin and Doherty suggested that the 25 K peak is also due to the Al-hole center. Martin et al.[26] were able to describe the broad loss as a single peak centered at about 135 K.

Figure 4 shows the acoustic loss, Q^{-1}, versus temperature spectrum for the Na-swept blank in the as-swept condition and after a room temperature irradiation. The irradiation has removed the large 55 K Al-Na^+ loss peak, while introducing the 25 K, 100 K, and 135 K peaks. The acoustic loss spectrum for the Li-swept sample after a room temperature irradiation is essentially the same as for the Na-swept sample. These three loss peaks are also observed in irradiated H-swept resonators fabricated from this same bar. However, their strength is reduced by approximately a factor of five. An inspection of the results reported by Doherty et al.[8] for the acoustic loss of their Na-swept resonator D14-45DC shows that the 25 K peak is small but present in their results. D14-45 series quartz has an aluminum content less than 1 ppm, so we would expect aluminum related loss peaks to be much smaller. Their Na loss peak is about 0.035 times that of our Na swept PQ-E resonator blank. It should also be noted that their resonator was partially H-swept. Thus, it appears that these three peaks, and the Na peak as well, scale with the aluminum content.

The thermal anneal behavior of the Al-hole and Al-OH^- centers in unswept quartz has been studied by Markes and Halliburton[7] and by Sibley et al.,[6] respectively. The Al-hole centers, as observed by ESR techniques, anneal out slightly below 300°C while the Al-OH^- center anneals out between 350°C and 400°C. These results strongly suggest that the alkali does not return to the aluminum site until the 350°C to 400°C range is reached. If the three radiation-induced loss peaks are due to the Al-hole center, they should show

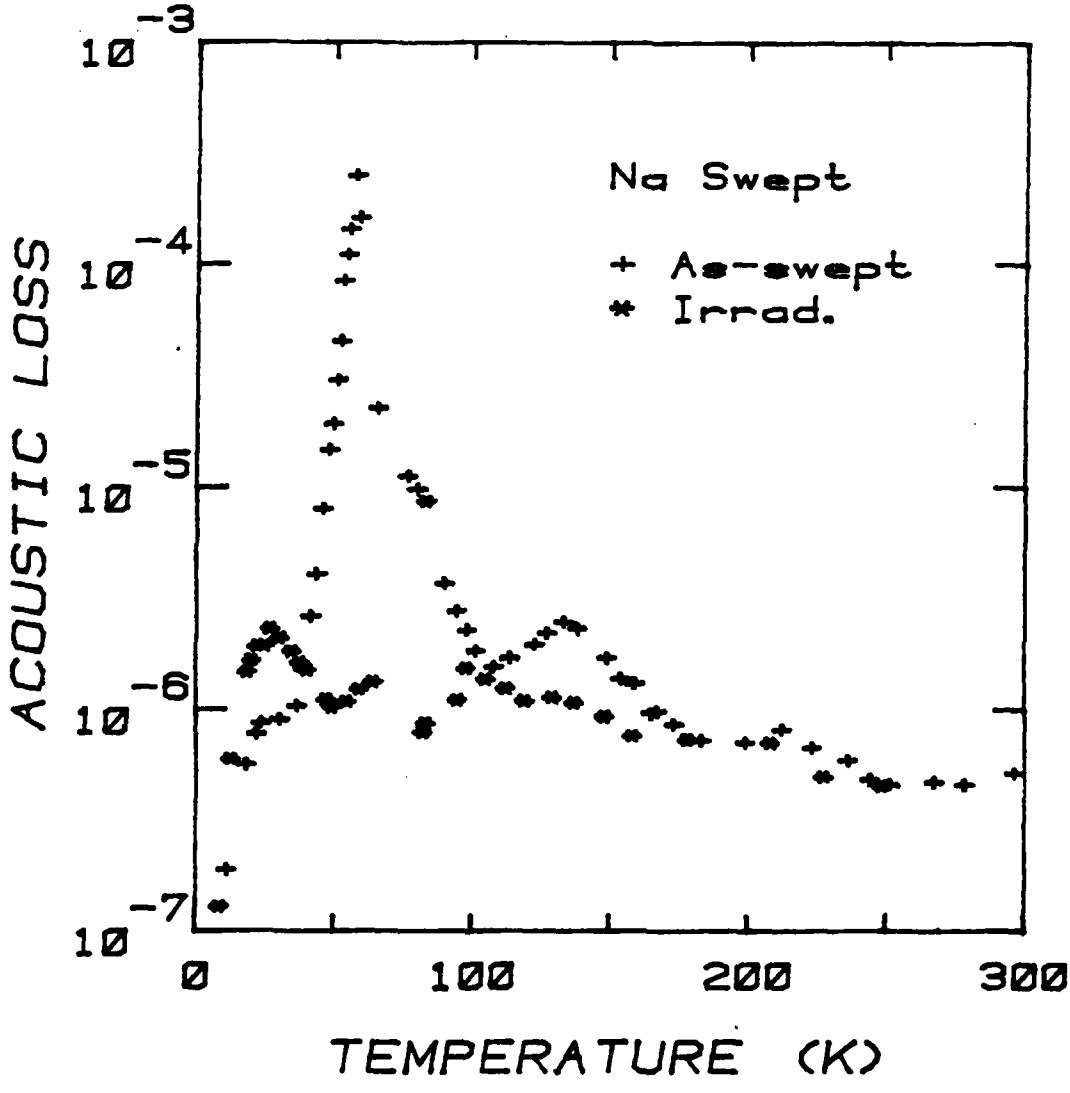

Figure 4. The acoustic loss spectrum of the Na swept resonator blank is shown for the as-received and irradiated conditions.

the same annealing pattern as the Al-hole center ESR spectrum. We have carried out an isochronal anneal study on the unswept blank and on the Li-swept blank. The results for the unswept blank show that the 25 K, 100 K, and 135 K loss peaks all anneal out at 270°C, as shown in Figure 4. Thus, all three loss peaks are most likely caused by the Al-hole center. When the anneal is continued to higher temperatures, the $Al\text{-}Na^+$ center loss peak recovers between 350°C and 400°C as shown in Figure 5. The thermal anneal of the $Al\text{-}OH^-$ center, as measured by infrared absorption, in a room temperature-irradiated unswept optical sample taken from the PQ-E bar is also shown in Figure 5. The $Al\text{-}OH^-$ strength grows slightly when the Al-hole centers decay and then goes out when the Na^+ ions return to the Al sites.

The isochronal anneal study also showed that after a room temperature irradiation and subsequent 400°C anneal, the 55 K $Al\text{-}Na^+$ peak in the unswept blank increased by approximately a factor of four (from 0.5×10^{-6} to 2.2×10^{-6}). The $Al\text{-}Na^+$ peak also appeared in the Li-swept sample as a result of annealing although it was absent in the as-Li-swept sample. These latter results suggest that Na is trapped at sites other than aluminum during the growth. The irradiation and anneal treatment just described evidently rearranged the alkalis within the sample. It is conceivable that this process would take place at the 50 to 80°C operating temperature of a crystal oscillator (although very slowly) and contribute to the long term aging of the crystal.

Often defect-related acoustic loss peaks can be described by

$$\Delta Q^{-1} = D\omega\tau / (1 + \omega^2\tau^2)$$

where ΔQ^{-1} is the loss above the intrinsic background, D is the strength factor, ω is the angular frequency, and τ is the relaxation time for reorientation of the defect. The relaxation is usually thermally activiated

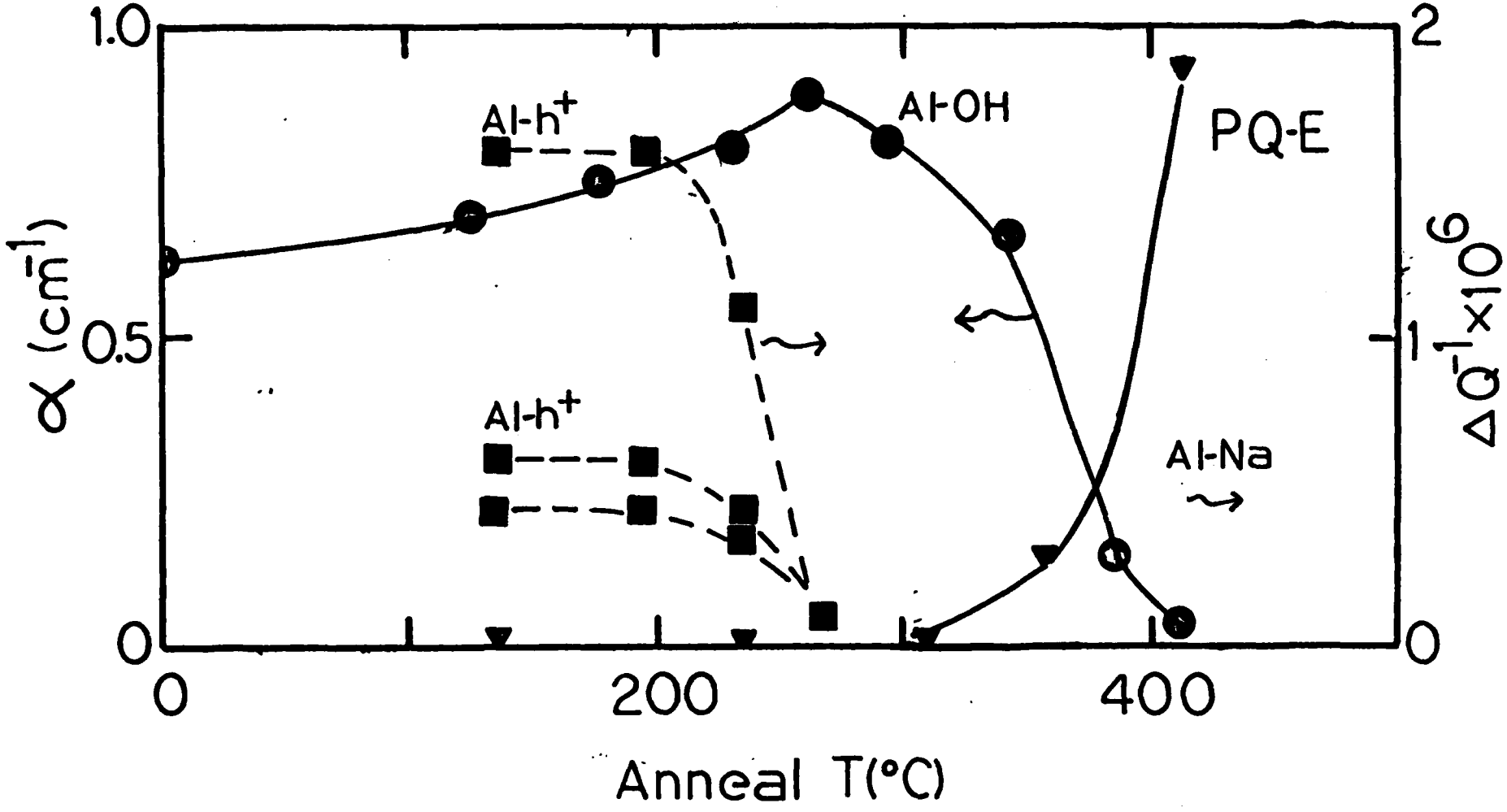

Figure 5. The isochronal anneal results for the Al-h^+ loss peaks, the Al-OH center and the Al-Na loss peak are shown for a resonator blank that was initially irradiated at 300 K.

as the defect must go over an energy barrier to reach the equivalent sites.[1] Thus,

$$\tau = \tau_0 \exp(E/kT)$$

where E is the barrier height and τ_0 contains the number of equivalent orientations and the attack rate. We have fit Eq. 1, with the relaxation time given by Eq. 2, to the 55 K and 135 K Aℓ-Na^+ center loss peaks and to the three radiation-induced Aℓ-h^+ peaks. The calculated parameters are given in Table II.

TABLE II. Loss Peak Parameters

T(K)	E(meV)	τ_0 (sec)	Defect
54	57	1.65×10^{-3}	Al-Na^+
135	130	4.44×10^{-13}	Al-Na^+
25	8	8.3×10^{-10}	Al-h^+
100	9	1.0×10^{-12}	Al-h^+
135	110	2.7×10^{-12}	Al-h^+

Our activation energies and relaxation times for the Al-Na^+ center are in good agreement with Park and Nowick's dielectric loss results,[23] as well as those of Stevels and Volger.[27]

Stevels and Volger have also reported a radiation-induced dielectric loss peak with E = 7.5 meV and $\tau_0 = 5 \times 10^{-7}$ sec. This activation energy is in reasonable agreement with our 25 K peak, but the relaxation time is much longer. Taylor and Farnell[28] have also made dielectric loss measurements on irradiated quartz; they found a loss peak near E = 7.5 meV in agreement with Stevels and Volger and an additional peak at low temperature with E = 1.2 meV and $\tau_0 = 6.2 \times 10^{-5}$s.

D. CONCLUSIONS

Sweeping Li^+, H^+, or D^+ into high-aluminum-content Premium Q grade quartz AT-cut resonators removes the small Al-Na^+ loss peak at 55 K but does not introduce any new loss peaks at temperatures below 370 K. Therefore, we conclude that the Al-Li^+ and Al-OH^- centers do not couple to the AT thickness shear mode. Na-swept samples show a very large 55 K loss peak. This shows that in as-grown quartz most of the Al sites are compensated by Li^+.

IV. X-RAY-INDUCED LUMINESCENCE

A. Introduction

Because of its multiple applications in electronic instrumentation, α-quartz has been widely studied in recent years. Much of this work has been directed toward understanding the effects of ionizing radiation.[1,5,19,20]

In the present section, we focus attention on the "blue" luminescence produced when quartz is exposed to ionizing radiation at low temperatures. Several tentative explanations of this emission have been proposed, but no definitive interpretation has yet emerged. Mattern et al.[31] studied the spectral distribution and the intensity of this "blue" emission as a function of temperature during ^{60}Co gamma-ray irradiation. The peak position was found to shift from 2.8 eV (440 nm) at 85 K to 3.2 eV (387 nm) at 210 K. To explain this large temperature effect, they suggested that the emission spectrum is actually composed of several bands with different thermal quenching properties. These authors numerically decomposed the emission spectrum at 85 K into four Gaussian-shaped curves and then tentatively proposed that the emission was due to the recombination of electrons with holes trapped at various aluminum sites.

Sigel[32] observed the "blue" luminescence during a study of transient optical absorption and emission effects in glassy and crystalline SiO_2.

During excitation of quartz at 4.2 K with a pulsed 500 keV electron source, he found an emission centered near 2.7 eV (460 nm). Also, this same electron excitation produced a transient optical absorption peaking at 215 nm. A similar steady-state ultraviolet absorption band had previously been assigned to oxygen vacancy defects[33] in the form of E' centers. Following an excitation pulse, the transient emission and absorption exhibit nearly the same time decay. This similarity prompted Sigel to suggest the "blue" luminescence arises from the radiative recombination of holes with electrons at E' center sites.

Trukhin and Plaudis[34] used vacuum-ultraviolet radiation, x-rays, and pulsed electrons to produce emission at 2.6 eV (477 nm) from quartz crystals maintained at 77 K. Through the use of polarization analyzers, they found that the luminescing centers are anisotropic in quartz. Their pulsed-electron experiments gave decay times at 77 K for the emission which are similar to the earlier results of Sigel.[32] Also, a rise time for the luminescence following a 20 nanosecond pulse was reported. These investigators proposed that the luminescence in quartz is intrinsic, i.e., excitons produced by the radiation break an Si-O bond and, thus, become self-localized excitons whose decay results in the luminescence. An additional study of the lunimescence produced by nanosecond pulses of electrons has been reported by Gritsenko et al.[35]

Griscom,[33] in a major review paper, states that the origin of the "blue" luminescence must still be regarded as an open question. In light of recent work in silica,[36] Griscom also introduces the possibility that this emission could arise at sites of O_2^{2-} peroxy linkages.[33]

With the goal of obtaining additional information about the responsible mechanisms, a systematic study of the spectral and temperature dependence of this "blue" emission from commercially available high-quality quartz crystals

is reported in this section. Different sample treatments including intense electron irradiation at room temperature, annealing to near the α-β phase transition, and electrodiffusion (sweeping) have been used to modify the luminescence characteristics. Our results show that the x-ray-induced luminescence consists of three overlapping bands, one which is suggested to result from electron recombination with holes trapped adjacent to Al-M^+ centers (where M^+ represents either Li^+ or Na^+) and two others which appear not to be associated with recombination near aluminum impurities.

B. Experimental

Quartz samples used in this investigation were obtained from two sources: Premium Q material purchased from Sawyer Research Products, Eastlake, Ohio and Supreme Q material provided by the Toyo Communication Equipment Company of Japan. Our study was restricted to Z-growth material because of its increased purity, and the sample labeling scheme introduced by Markes and Halliburton[7] has been followed. A Toyo sample from bar SQ-A was swept in a hydrogen atmosphere at Oklahoma State University. All irradiations, exclusive of the luminescence excitations, were with electrons from a Van de Graaff accelerator (1.7 MeV and 0.2 μA on the sample).

Luminescence in the quartz was excited with x-rays from a Machlett OEG-60 tube (a tungsten target and a 1.5 mm thick beryllium exit window) operating at 50 KV and 30 mA. The sample was attached by a copper clamp to the cold finger of a home-built cryostat. Emitted light was dispersed by a 0.25 m Spex monochromator with grating blazed at 300 nm and was detected by an RCA C31034 photomultiplier tube. No instrumental spectral response corrections have been made to the data presented in this paper. For measurements of the temperature dependence of the emitted-light intensity, the sample was heated at a linear rate of 10 K/min. Both the total light output and the light emitted at specific wavelengths were detected as a function of temperature.

C. Results

The spectral dependence of the x-ray-induced "blue" emission from α-quartz depends on previous sample treament. We illustrate this first by describing results from unswept sample PQO-E18 in considerable detail, and then by presenting later in this section results from unswept sample SQO-A3 and swept sample SQ-A4. The behavior reported for these particular samples is believed to be characteristic of all high-quality synthetic quartz commercially available today.

At 80 K, an unswept sample with no prior irradiation (i.e., as-grown) emits a broad band centered at about 430 nm with a half-width of 0.77 eV. This band is shown by the solid curve in Fig. 6. If the same sample has been heavily electron irradiated (to a dose of approximately 10^7 rad) at room temperature, the subsequent x-ray-induced emission spectrum at 80 K is also a band peaked at 430 nm but with a half-width of 0.69 eV. This latter emission, normalized to the same intensity, is shown by the dashed curve in Fig. 6. The main change in the shape of the emission band after the room-temperature electron irradiation takes place in the high energy wing and, although not great, is easily observable.

An unswept sample that has been electron irradiated at room temperature but then annealed at temperatures near 750 K show the same emission band at 80 K as a sample with no previous irradiation. More generally, we have found that an unswept sample can be repeatedly cycled from emitting the 0.77 eV half-width band to emitting the 0.69 eV half-width band by sequentially annealing at 750 K and electron irradiating at room temperature. In the remainder of the section, we will refer to these two states, or conditions, of the quartz crystal as "annealed" and "room-temperature-irradiated".

Although x-rays cause significant visible emission from quartz at 80 K, no emission is observed during similar excitation at room temperature. In

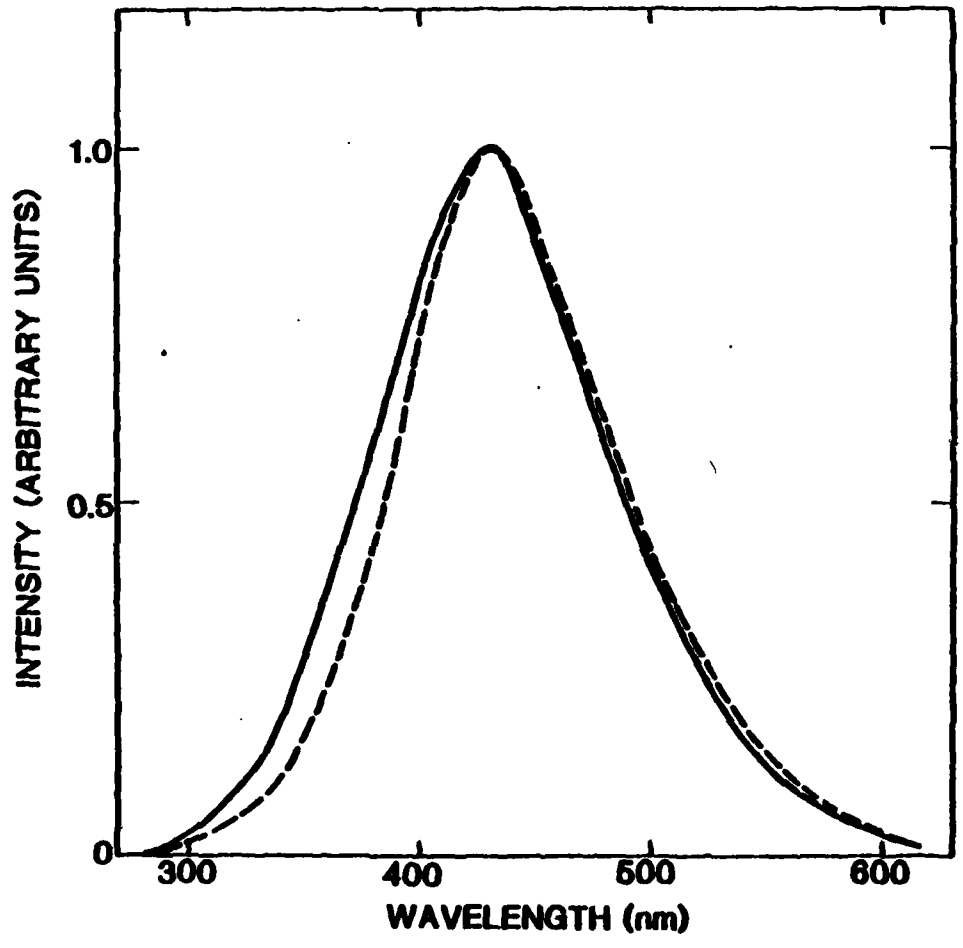

Figure 6. X-ray-induced emission spectrum from quartz sample PQ-E18 measured at 80 K. The solid curve was obtained from the as-received sample while the dashed curve was taken after an intense electron irradiation at room temperature.

order to characterize this thermal quenching in more detail, the total emitted light was recorded as a function of temperature in the 80-295 K range. These results are plotted in Fig. 7 for an annealed sample (0.77 eV half-width emission band) and in Fig. 8 for a room-temperature-irradiated sample (0.69 eV half-width emission band). In the case of the annealed sample, the thermal quenching takes place in three stages. These are labeled Stage I (120-160 K), Stage II (170-210 K), and Stage III (220-270 K). For the room-temperature-irradiated sample, Stage III is missing but Stage I and Stage II are present. The temperature dependence of the emitted light at selected wavelengths is shown in Fig. 9 for an annealed sample. These curves show the same three stages as Fig. 7 but the relative contribution to each stage is seen to depend strongly on the wavelength.

An analysis of the temperature dependence of the emission intensity reveals that each quenching stage can be fit to an equation of the form

$$\eta = \frac{1}{1 + \frac{s}{b} e^{-E/kT}} .$$

This equation describes the competition between radiative and non-radiative decay and corresponds to the classical expression for the emission quantum yield.[31] In Eq. (3), s is the "attempt" frequency and E is the activation energy for the thermally activated non-radiative decay while b is the transition rate for the radiative decay. The sets of data illustrated by the dashed curves in Figs. 7 and 8 were used to make graphs of $\ln[\eta/(1-\eta)]$ versus 1/T. Although not shown, this resulted in a series of linear plots from which values of s/b and E corresponding to each thermal quenching stage were obtained. These parameters are given in Table III. Stages I and II gave the same values in the annealed and the room-temperature-irradiated samples.

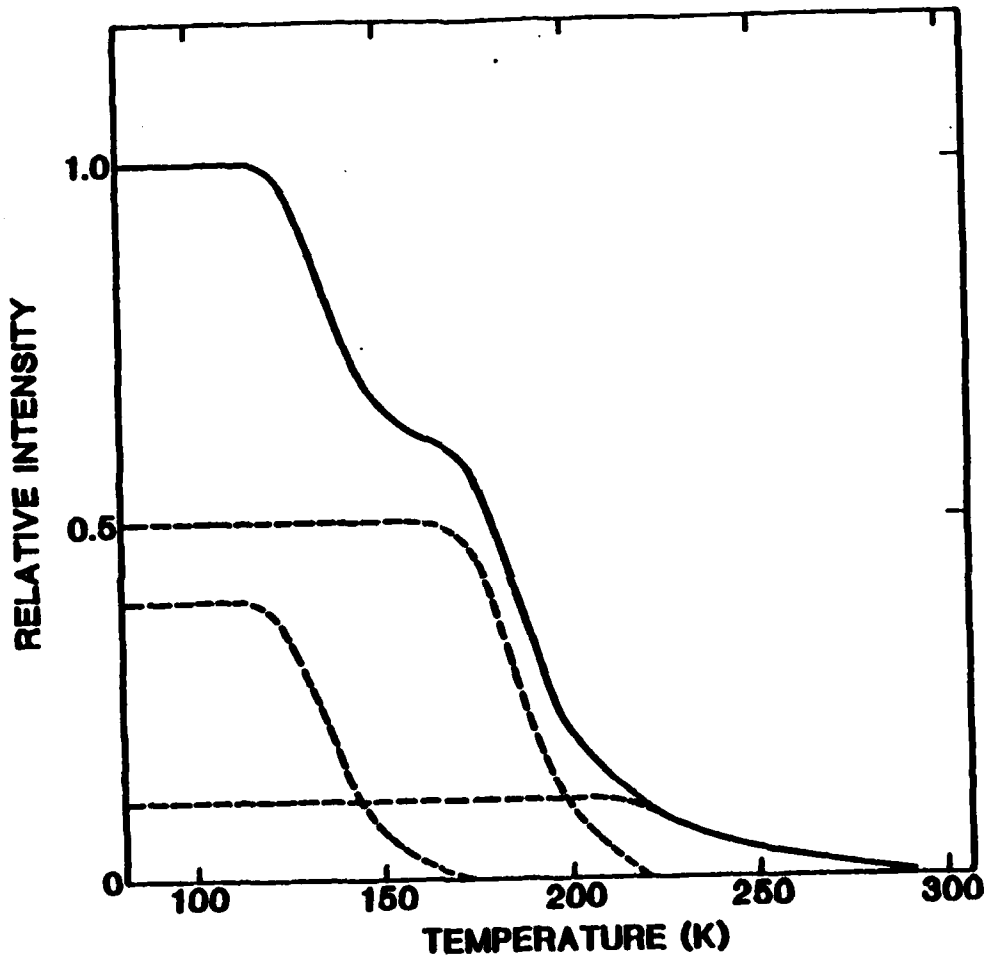

Figure 7. Temperature dependence of the total emitted light (solid curve) during x-ray excitation of sample PQ-E18 after a thermal anneal near 750 K. Similar results are obtained from as-grown samples. The dashed curves represent the relative contribution of each thermally-quenched band to the total emitting light at each temperature.

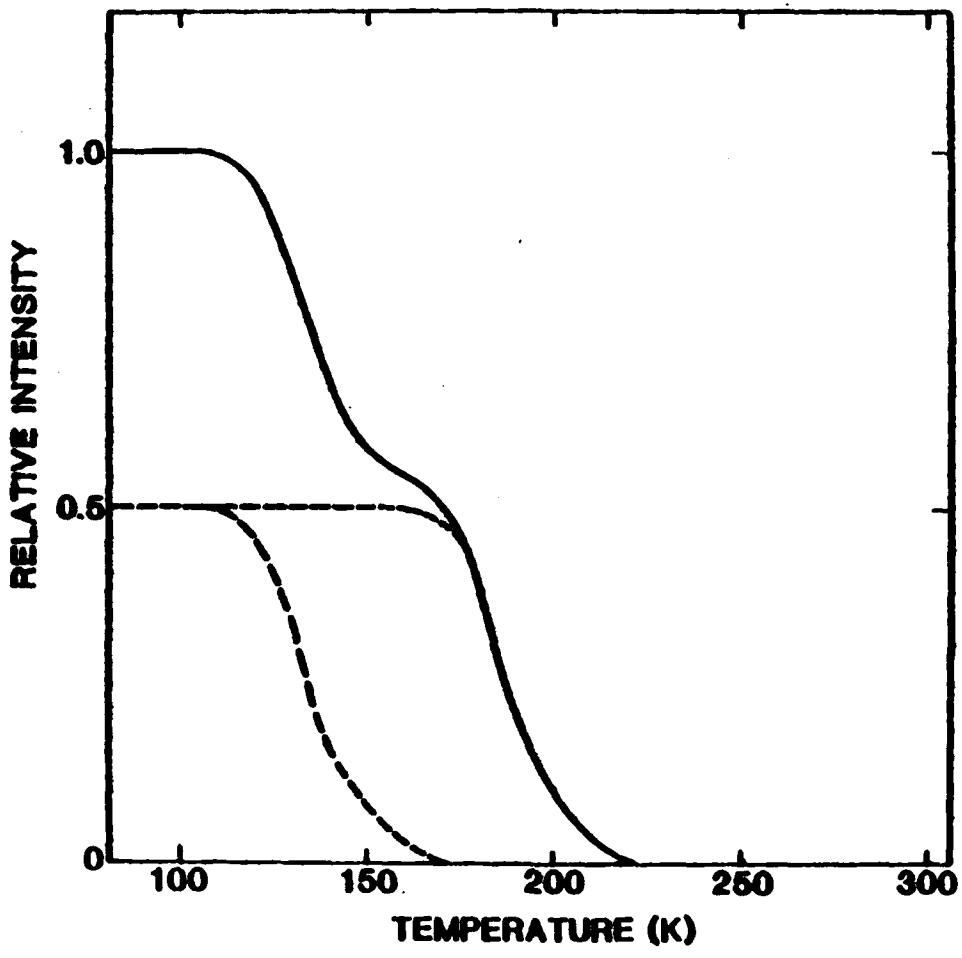

Figure 8. Temperature dependence of the total emitted light (solid curve) during x-ray excitation of sample PQ-E18 after an intense electron irradiation at room temperature. The dashed curves represent the relative contribution of each thermally-quenched band to the total emitted light at each temperature.

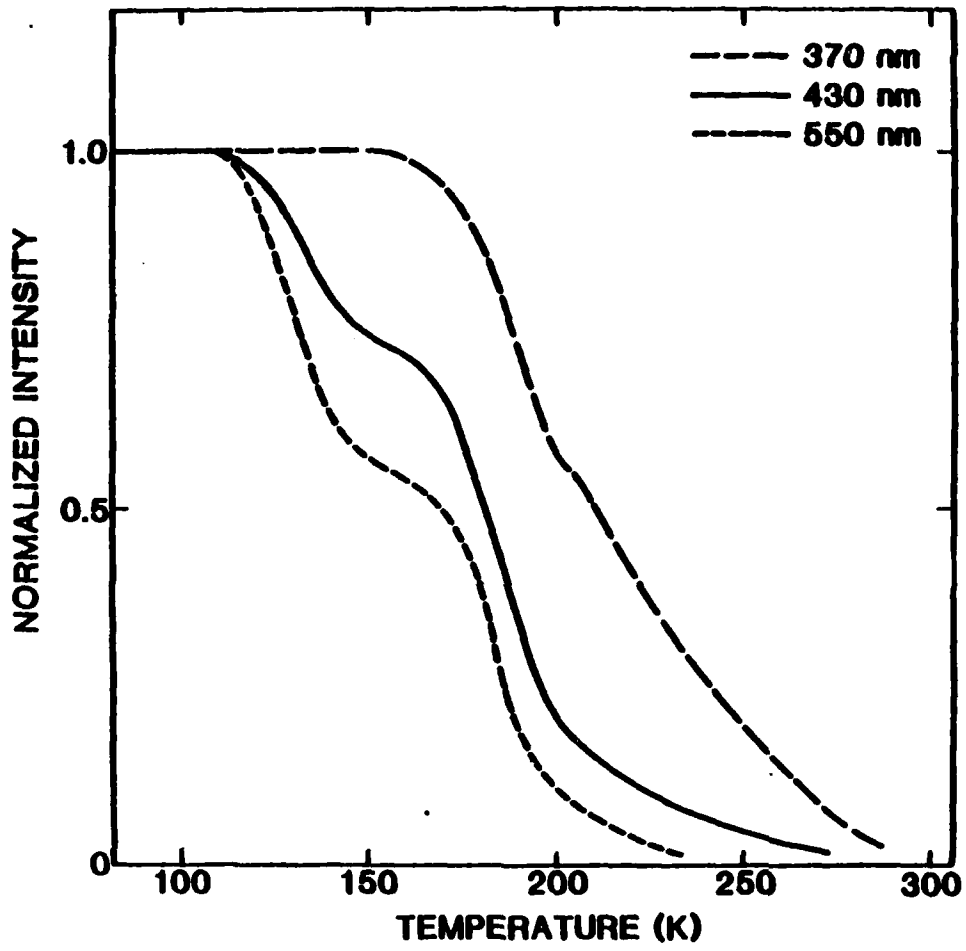

Figure 9. Temperature dependence of the emitted light at specific wavelengths during x-ray excitation of annealed sample PQ-E18.

The thermal quenching results indicate that the observed emission is composed of bands; three in the case of an annealed sample and two in the case of a room-temperature-irradiated sample. With the goal of experimentally resolving the individual bands in the low temperature x-ray-induced emission, measurements of the spectral dependence were made at 80 K, 160 K, and 225 K. The results are shown in Fig. 10 for an annealed sample and in Fig. 11 for a room-temperature-irradiated sample. At these specific temperatures, either none, one, or two of the bands are quenched.

Only one band remains unquenched at 225 K in an annealed sample and is represented by curve A in Fig. 10. Curve B in Fig. 10 was taken at 160 K and represents the sum of the two bands which remain unquenched at this temperature. Finally, curve C was taken at 80 K and represents the sum of all three bands; it is the same as the solid curve in Fig. 6. On the other hand, in Fig. 11 no emission is found at 225 K since the one band which remains unquenched at this temperature in an annealed sample does not occur in a room-temperature-irradiated sample. Curve D in Fig. 11 represents the one band which remains unquenched at 160 K in this type of sample. Curve E in Fig. 11 was taken at 80 K and represents the sum of two bands; it is the same as the dashed curve in Fig. 6.

The curves in Figs. 10 and 11 provide sufficient information to determine the individual shapes of the three bands contributing to the total "blue" luminescence in quartz. Each of the three bands and their relative intensity contribution are shown in Fig. 12 for an annealed sample. They were obtained by the following procedure. First, Band III is simply curve A in Fig. 10. Band II is obtained by taking the difference between curves A and B in Fig. 10 or by simply taking curve D in Fig. 11. Band I is the difference between curves B and C in Fig. 10 or, equivalently, the difference between curves D and E in Fig. 11. The peak positions and half-widths of these simpler

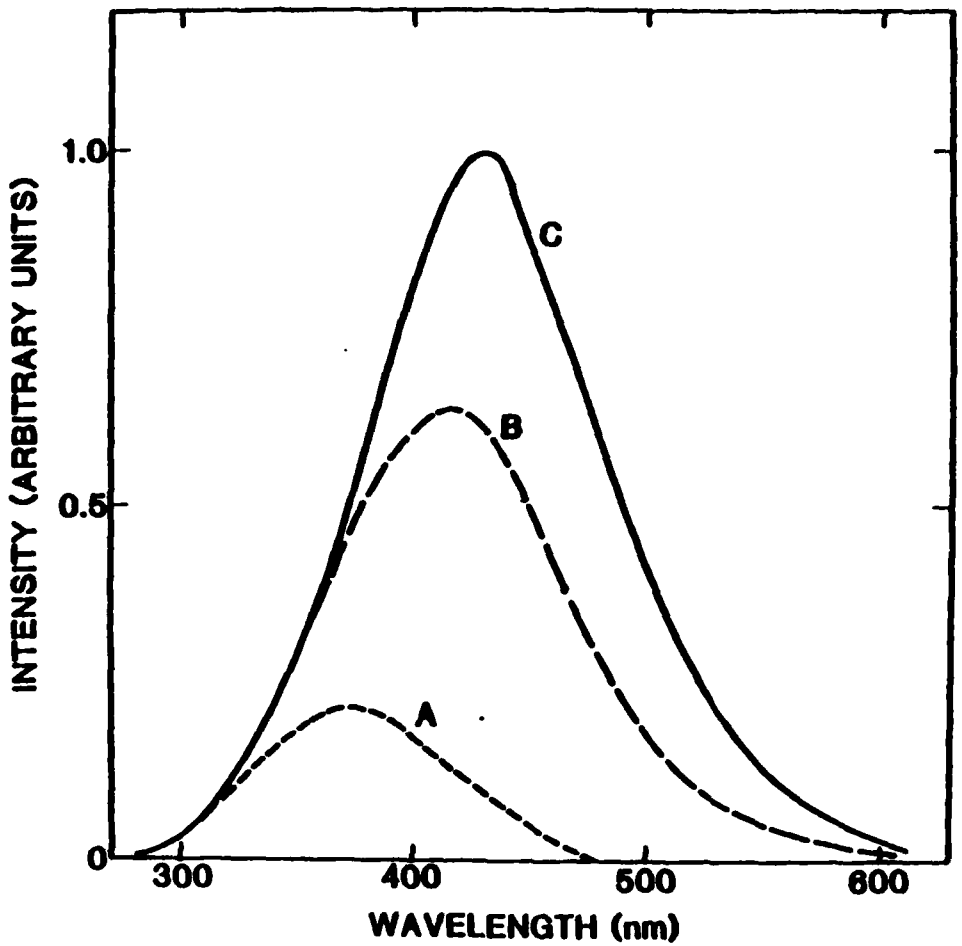

Figure 10. X-ray-induced spectrum from annealed sample PQ-E18 taken at the following temperatures; 225 K for curve A, 160 K for curve B, and 80 K for curve C.

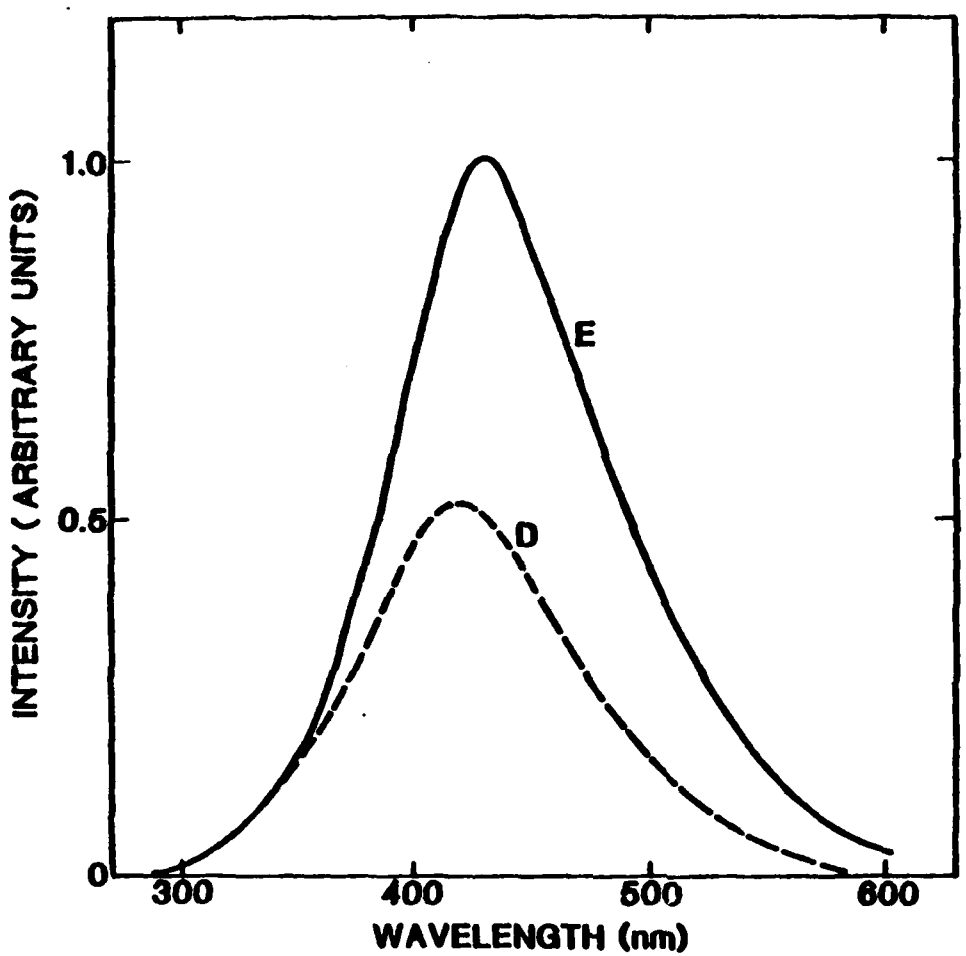

Figure 11. X-ray-induced spectrum from room-temperature-irradiated sample PQ-E18 taken at the following temperatures; 160 K for curve D and 80 K for curve E.

resolved bands are given in Table IV. As shown in Fig. 12, the sum of Bands I, II, and III give a curve which is the same as the solid curve in Fig. 6. The total emission from a room-temperature-irradiated sample, corresponding to the dashed curve in Fig. 6, can be resolved into only Bands I and II. The primary assumption in our process of resolving the individual bands has been that there are no temperature-induced changes in their peak positions and shapes. Although this most likely is is not absolutely true, it is expected to be a good approximation since only very slight shifts in peak position with temperature have been observed for similar emissions in other materials.

Table III Parameters characterizing the thermal quenching of each of the three stages found in the "blue" emission of quartz.

Stage	s/b	E(eV)
I	6.30×10^7	0.21
II	2.62×10^{12}	0.43
III	1.47×10^7	0.35

Table IV. Peak positions (λ_m) and half-widths (W) of the three resolved bands.

	λ_m	W
Band I	440 nm (2.82 eV)	0.64 eV
Band II	425 nm (2.92 eV)	0.75 eV
Band III	380 nm (3.26 eV)	0.92 eV

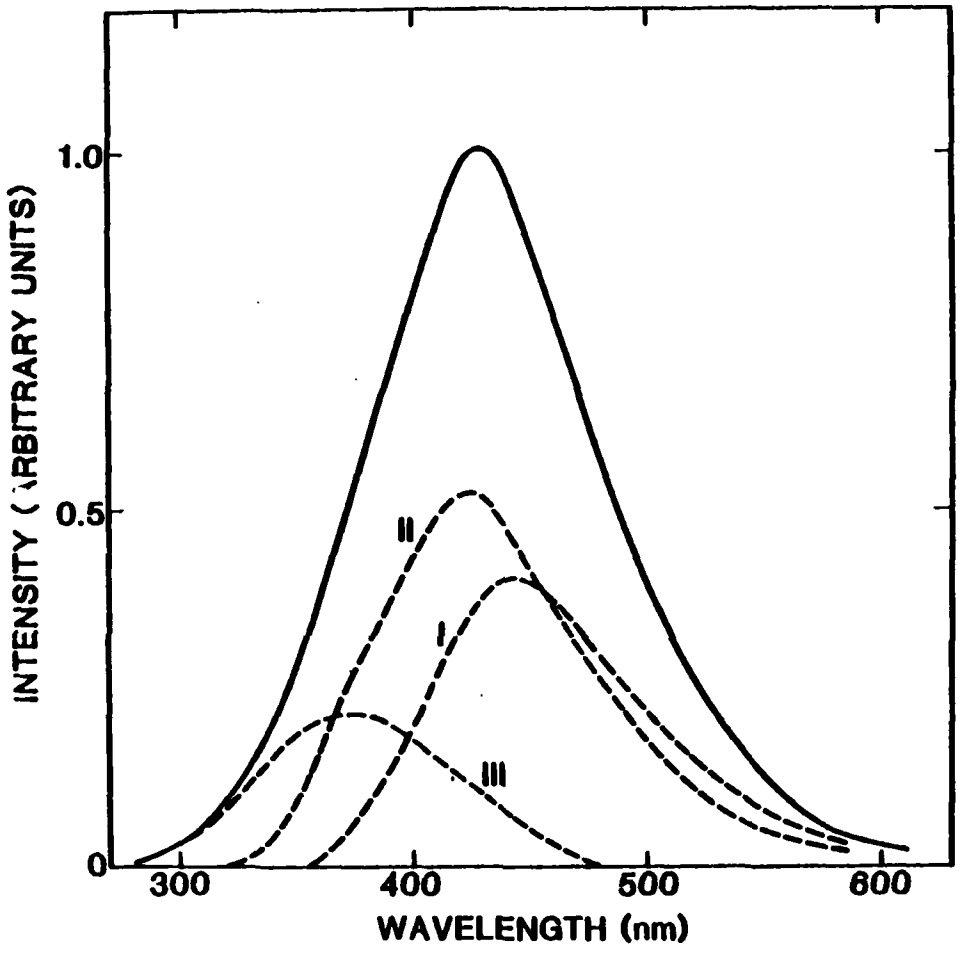

Figure 12. The solid curve represents the total "blue" emission in quartz and the dashed curves represent the three component bands and their relative contributions.

An additional experiment with an unswept sample was designed to determine the effect of pre-existing aluminum-hole centers, known as $[Al_{e+}]^{\circ}$ centers, on the x-ray-induced emission. First, the sample was subjected to an intense electron irradiation at room temperature followed by a similar intense electron irradiation at 80 K. Without warming the sample, the x-ray-induced emission spectrum was obtained. Then the sample was allowed to warm to room temperature for several minutes before being returned to 80 K where the x-ray-induced emission spectrum was taken again. The two emission spectra are shown in Fig. 13. A large concentration of aluminum-hole centers were created by the intense electron irradiation at 80 K and were present during the taking of the first x-ray-induced spectrum, but the anneal to room temperature destroyed approximately one-third of these aluminum-hole centers[5,7] and meant that fewer such centers were present during the taking of the second x-ray-induced spectrum. As shown in Fig. 13, an increase of about 25% in the intensity of the x-ray-induced emission at 80 K coincides with the decrease in the number of aluminum-hole centers in the sample.

Besides the unswept Sawyer Premium Q sample (from bar PQ-E) already described, Supreme Q samples from Toyo were also studied. Two samples were cut from adjacent positions in the unswept Toyo bar SQ-A. One of these, labeled SQ-A3, was left unswept while the other, labeled SQ-A4, was swept in a hydrogen atmosphere, thus removing all alkali interstitials. Not surprisingly, it was found that the x-ray-induced luminescence of sample SQ-A3 was the same, in all respects, as sample PQ-E18. The similarities included the changing from an emission band of 0.77 eV half-width for either an as-grown sample or after a 750 K thermal anneal to a band of 0.69 eV half-width after an intense room-temperature irradiation. Also, the temperature dependence of the emitted light intensity corresponded exactly with that reported for sample PQ-E18, showing all three stages.

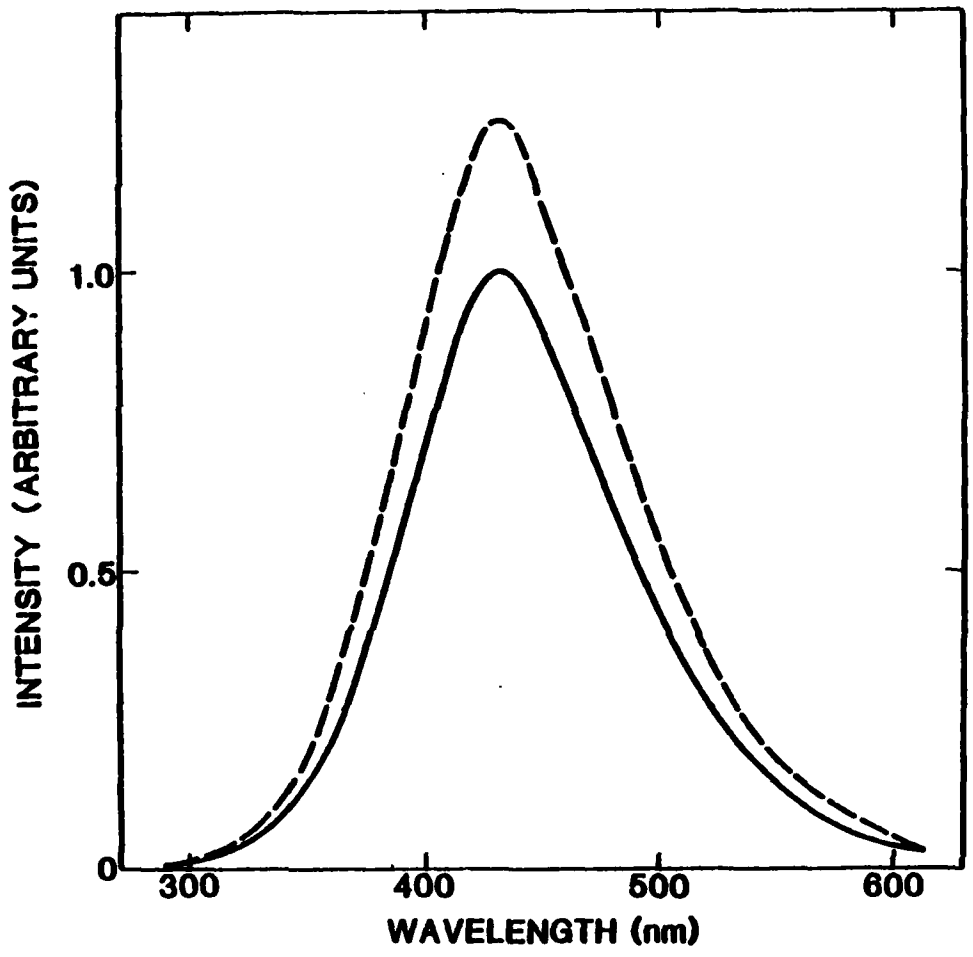

Figure 13. These two x-ray-induced luminescence spectra were taken at 80 K from the same sample. The difference is that approximately 50% more pre-existing aluminum-hole centers were present when the solid curve was taken.

The hydrogen-swept sample SQ-A4, however, behaved in a manner somewhat different from the unswept samples. The half-width of the x-ray-induced luminescence band from the swept sample was always 0.69 eV. This was the case whether the sample had been annealed near 750 K or heavily electron irradiated at room temperature. It was found that the temperature dependence of the emitted light from the swept sample showed only the Stages I and II, never Stage III.

D. Discussion

In our present investigation, the x-ray-induced "blue" luminescence from quartz has been experimentally resolved into three overlapping bands, each having a different quenching temperature. These results (1) correlate well with data from a previous thermoluminescence study; (2) lead to a possible model for the origin of one of the three emission bands; and (3) form the basis of an optical test for measuring the effectivness of sweeping of quartz crystals.

In the thermoluminescence (TSL) study of high-quality quartz by Malik et al.,[37] three regions of glow peak interest were identified below room temperature, occuring as follows: Region I (115-145 K), Region II (145-185), and Region III (185-270 K). Definite similarities are found between their TSL data and the present x-ray-induced lunminescence data. Region I in the TSL contains a single, sharp peak at 128 K with the maximum in the spectral emission being near 450 nm. This is similar to our Band I whose emission peak is at 440 nm and whose thermal quenching begins at about 120 K. Although the significance is not yet understood, it is very interesting nonetheless that the TSL peak in Region I, the onset of thermal quenching of Band I, and the thermal decay of radiation-induced hydrogen atom defects[7] all occur in the 120-130 K range.

Region III in the TSL study by Malik et al.[37] contains a single peak near 225-230 K which has a spectral emission maximum near 380 nm. Our Band III emission peaks at 380 nm and its thermal quenching begins at about 220 K. However, the most striking correlation between the Region III TSL peak and our Band III is that neither occurs in swept quartz or in unswept quartz heavily irradiated at room temperature and not subsequently annealed. In other words, this TSL peak and Band III are observed only when interstitial alkali ions are in the crystal and located adjacent to substitutional aluminum ions.

In order to explain the origin of Band III, two additional observations must be considered. First, the temperature dependence of the intensity of Band III (i.e., the thermal quenching) in an annealed unswept sample correlates well with previous data relating to the temperature dependence of the radiation-induced mobility of interstitial alkali ions, as shown in Fig. 14. Markes and Halliburton[7] and Halliburton et al.[5] have shown that the sample temperature must be about 200 K before ionizing radiation can begin to free interstitial alkalis from their trapping site adjacent to alunminum ions. The dashed curve in Fig. 14 represents the production of aluminum-hole (Al-h^+) centers as the interstitial alkali ions are removed from the aluminum sites by radiation.[5]

The other important evidence comes from Ge-doped quartz where Mackey[38] has directly observed the thermal dissociation of the h^+-Al-M^+ center (also known as the [Al_e+/M^+] center where the symbol M^+ represents Li^+ or Na^+) into a separate Al-h^+ center and an M^+ ion. The Ge^{4+} ions act as electron traps below 200 K and allow stable h^+-Al-M^+ centers to be formed by radiation, which

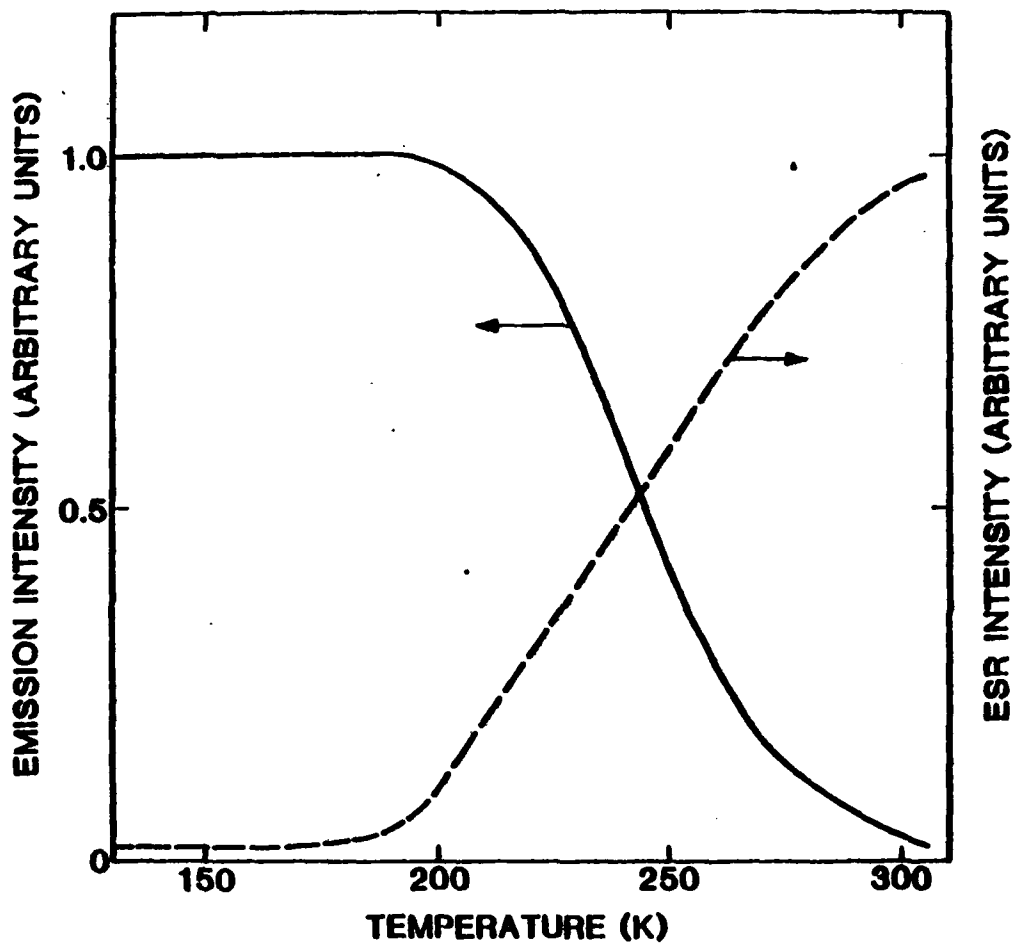

Figure 14. Comparison of the thermal quenching of Band III (solid curve) with the radiation-induced mobility of interstitial alkali ions (dashed curve). The dashed curve is electron spin resonance (ESR) data from Reference 4.

then begin to dissociate upon warming above 200 K. The M^+ ion leaves the $Al-h^+$ center behind and thermally migrates to the Ge^{3+} ions. In the undoped quartz used in the present investigtion, there are no electron traps known which play the analogous role of the Ge^{4+} ions and, as a result, no significant number of stable $h+Al-M^+$ centers are observed by electron spin resonance (ESR) after electron irradiation at 77 K.

These three observations, namely (1) the emission band only occurs when alkalis are adjacent to aluminum ions, (2) thermal quenching of the band correlates with the radiation-induced mobility of alkalis, and (3) h^+-Al-M^+ centers thermally dissociate above 200 K in Ge-doped quartz, suggest the following model for the origin of Band III in our samples. Radiation produces large numbers of uncorrelated electron-hole pairs in quartz and some of the holes become temporarily trapped on oxygen ions adjacent to $Al-M^+$ centers. This formation of h^+-l-M^+ centers is followed by one of two possible events, depending on the temperature. Below 200 K, the electron finds no stable trapping site and hence returns and recombines with the hole at the h^+-Al-M^+ center to give a luminescence. Above 200 K, the thermal energy becomes sufficient to allow the alkali ion (i.e., the M^+ ion) to "hop" away from the remaining $Al-h^+$ center before the return of the electron. This latter happening leaves no h^+-l-M^+ center at which recombination can occur, and no comparable emission is observed.

Thus, we are proposing that the Band III emission arises from recombination of an electron with a hole trapped adjacent to an $Al-M^+$ center, and the thermal quenching of the band reflects the thermal destruction of the h^+-Al-M^+ center before the electron can return and recombine. The lack of alkali ions in the swept samples eliminates this source of emission and agrees with our failure to observe a contribution from Band III in such samples.

Besides providing a more fundamental understanding of the radiation response of α-quartz, the present investigation also has practical application with regard to testing of sweeping effectiveness. As shown earlier, Band III is related to the presence of alkali-compensated aluminum ions (i.e., $Al\text{-}M^+$ centers), and a measurement of the emitted light intensity in the 220-270 K temperature range provides information about the concentration of these alkali-compensated aluminum ions. Similar information also can be obtained from measuring the intensity of the Region III thermoluminescence, as described by Malik et al.[37]

A test for sweeping effectiveness would be to monitor the x-ray-induced luminescence at 370 nm and at approximately 250 K from a sample before and after sweeping. The choice of 370 nm for the monitoring wavelength optimizes the observance of Band III emission as opposed to the contributions from Bands I and II. If the intensity of the x-ray excitation beam is sufficiently great, the ratio of the luminescence intensity found after the sweep to that found before the sweep would give the percentage of alkali ions remaining in the sample after sweeping. If all the alkalis are removed by the sweep then the luminescence intensity at 250 K is zero after the sweep and the sample is said to be 100% swept. An example of data supporting our proposed luminescence test procedure is given in Fig. 15 where the x-ray-induced luminescence measured at 370 nm from unswept annealed sample SQ-A3 (dashed curve) is compared to that from swept sample SQ-A4 (solid curve.) The emission intensity from the unswept sample is much larger at 250 K than that from the swept sample at this temperature, which indicates the latter sample is well-swept and has no Band III.

With regard to selecting quartz for use in precision frequency control applications, a single luminescence measurement of the type described above,

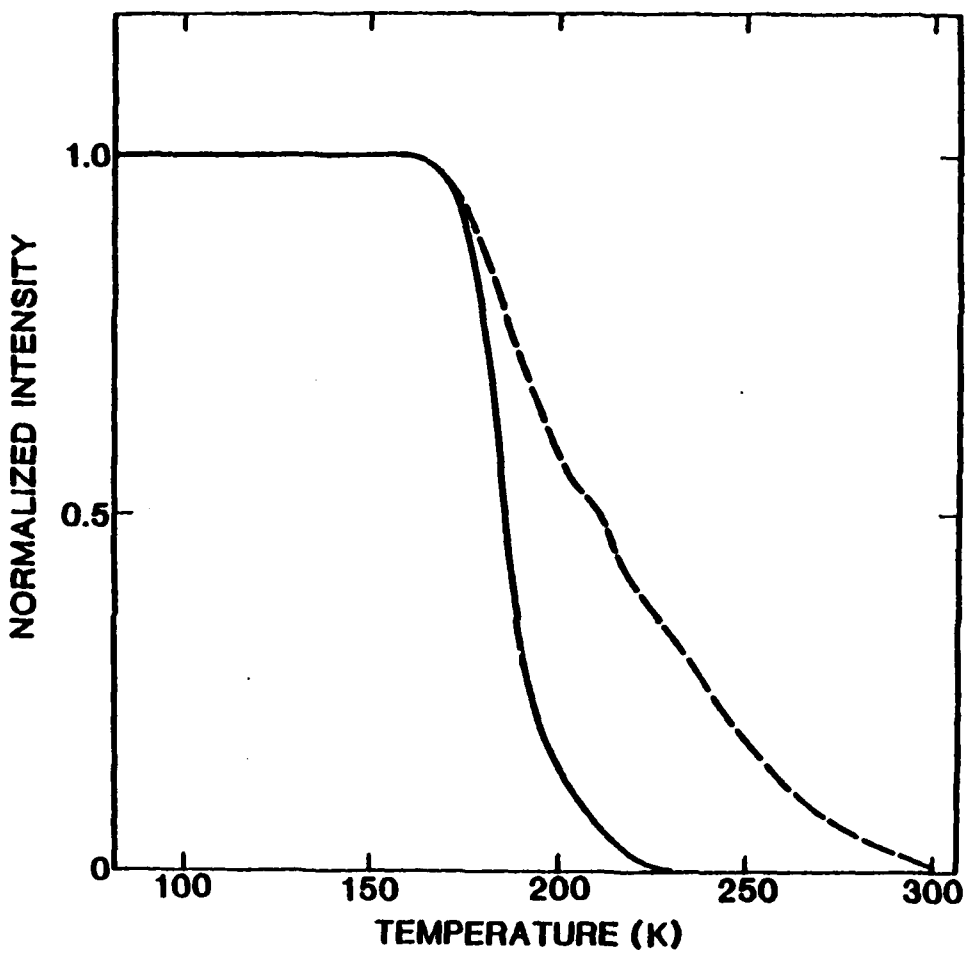

Figure 15. Comparison of x-ray-induced luminescence as a function of temperature from an unswept annealed sample (dashed curve) and a swept sample (solid curve).

if done on as-grown material, could be used as an initial screening test since it would provide a value for the $Al-M^+$ center concentration. Only those bars having $Al-M^+$ concentrations below a pre-set acceptable value should be subjected to sweeping or other processing. A screening test for material already swept could also consist of making a single measurement of the type described above. In this case, quartz exhibiting a luminescence intensity above a pre-set value would either not be well swept or would contain a large concentration of aluminun (the single measurement could not distinguish between the two explanations), and, in either case, should be rejected from further processing.

E. Summary

Our experimental studies have provided considerable information about the x-ray-induced "blue" emission from synthetic quartz. The major results are sunmmarized by the following statements. (1) In as-grown crystals the emission obtained by excitation at 80 K is peaked near 430 nm with a half-width of 0.77 eV. It is thermally quenched in three stages and has been experimentally resolved into three simpler overlapping bands peaking at 440 nm, 425 nm, and 380 nm. (2) If the crystal has received a previous intense electron irradiation at room temperature, the emission produced by excitation at 80 K appears narrower (half-width of 0.69 eV) and it is thermally quenched in only two stages. This latter emission is resolved into two simpler bands peaking at 440 nm and 425 nm. (3) If a room-temperature-irradiated sample has been annealed at temperatures above 750 K, it shows the same behavior as an as-grown sample. (4) If a sample has been swept in a hydrogen (or air) atmosphere, the emission does not change with sample treatment and always coincides with that of the unswept sample after room temperature irradiation.

From these results, we conclude that the band which peaks at 380 nm probably arises from recombination of an electron with a hole trapped adjacent to an Al-M^+ center. This particular band is only observed when interstitial alkali ions are in the crystal and are trapped next to the substitutional aluminum ions. The origins of the other two bands at 440 nm and 425 nm are not revealed in this study, although data suggests they do not arise from electron-hole recombination near aluminum ions. Finally, the behavior of the 380 nm band is proposed as the basis of a test for use in screening quartz bars prior to fabrication of resonators designated for precision frequency applications.

V. RADIATION-INDUCED E' CENTERS

A. Introduction

In quartz, an important class of radiation-induced paramagnetic defects have g values slightly less than 2.0023 and have very long spin-lattice-relaxation times. The best known of these defects is the E'_1 center. first reported by Weeks [39] and further characterized by Silsbee [40]. Theoretical investigations by Feigl et al. [41] and Yip and Fowler [42] have led to the presently accepted model of the E'_1 center; namely, an oxygen vacancy with an associated unpaired electron. This unpaired electron is localized in an sp^3 hybrid orbital extending into the vacancy from the adjacent silicon ion on the short-bond side of the vacancy. The precursor of the E'_1 center has not been identified.

Similar oxygen-vacancy-associated defects involving hydrogen are known as E'_2 and and E'_4 centers. [43-47] An extensive analysis of the E'_1 center by Isoya et al. [48] has resulted in a model simply described as an H^- ion in an oxygen

vacancy along with an unpaired electron which is shared unequally by the two neighboring silicon ions. In the case of the E_1' center, no definitive model has been proposed.

In the present section, we describe three radiation-induced S = 1 centers in quartz which we have labeled E_1'', E_2'', and E_3''. These centers are very similar to the E_1' center, and we use a notation consistent with that of the E_1' wherein the number of primes donotes how many unpaired electrons a center possesses. [49] Weeks and Abraham [50,51] first reported these S = 1 centers and they were briefly described by Solntsev et al. [52] We have extended these initial observations by using electron spin resonance (ESR) to examine both unswept and hydrogen-swept samples of commercially available high-quality synthetic quartz. This work provides a more detailed description of the production and thermal decay properties of these E'' centers.

B. Experimental

Synthetic quartz was obtained from Sawyer Research Products, Eastlake, Ohio, USA and from Toyo Communications Equipment Company, Japan. These were lumbered bars of pure Z-growth material from which Y plates (8x3x12 mm^3) were cut for use in the ESR studies. A van de Graaff accelerator (1.7 MeV electrons) was used for all irradiations; the samples were immersed in liquid nitrogen for the irradiations at 77 K while nitrogen gas of the desired temperature flowed by the sample during the irradiations between 77 K and 300 K. All of the ESR spectra described in this paper were taken at room temperature.

The homodyne ESR spectrometer utilize a microwave bridge of our own design operating at X-band and containing a detector bias arm. A Narda N6244S-37 microwave solid-state amplifier was added to the bridge to increase sensitivity especially at lower microwave power. The static magnetic field

modulation frequency was 100 kHz. A variable-temperature nitrogen gas flow permitted thermal anneal studies up to 200°C within the microwave cavity. Magnetic field positions and g values were measured with a Varian E-500 digital gaussmeter and an HP-5340A microwave frequency counter.

C. Results

The Three E'' centers are easily produced in unswept synthetic quartz by an electron irradiation at 77 K, provided the sample has been previously irradiated at room temperature and not subsequently annealed at high temperatures (i.e., above 600-750 K). In contrast, a single 77 K electron irradiation of a previously unirradiated unswept sample does not produce appreciable numbers of E'' centers. Because of long spin-lattice-relaxation times, the ESR spectra of the E'' centers are most readily observed at room temperature. The ESR spectrum showing the E_1'', E_2'', and E_3'' centers when the magnetic field is oriented along the crystal's c axis is given in Fig. 16. In all cases, the intensities of the three E'' centers are found to be in the ratio 4.5:2:1 following a 77 K irradiation.

At room temperature, the centers are found to power saturate easily, even at microwave levels less than 0.2 milliwatts. This allows complex passage effects to occur within the E'' spin systems and required that the ESR spectrometer's 100 kHz phase-sensitive detector be adjusted "out-of-phase" in order to optimize the intensity of the ESR signals. Since the ESR linewidths for these centers are extremely narrow, less than 0.05 gauss, this phase setting also prevents modulation "sidebands" from appearing and giving distorted ESR lineshapes.

As seen in Fig. 16, each of the three E'' centers exhibits a pair of intense ESR lines. These doublets are, in turn, surrounded by smaller ^{29}Si

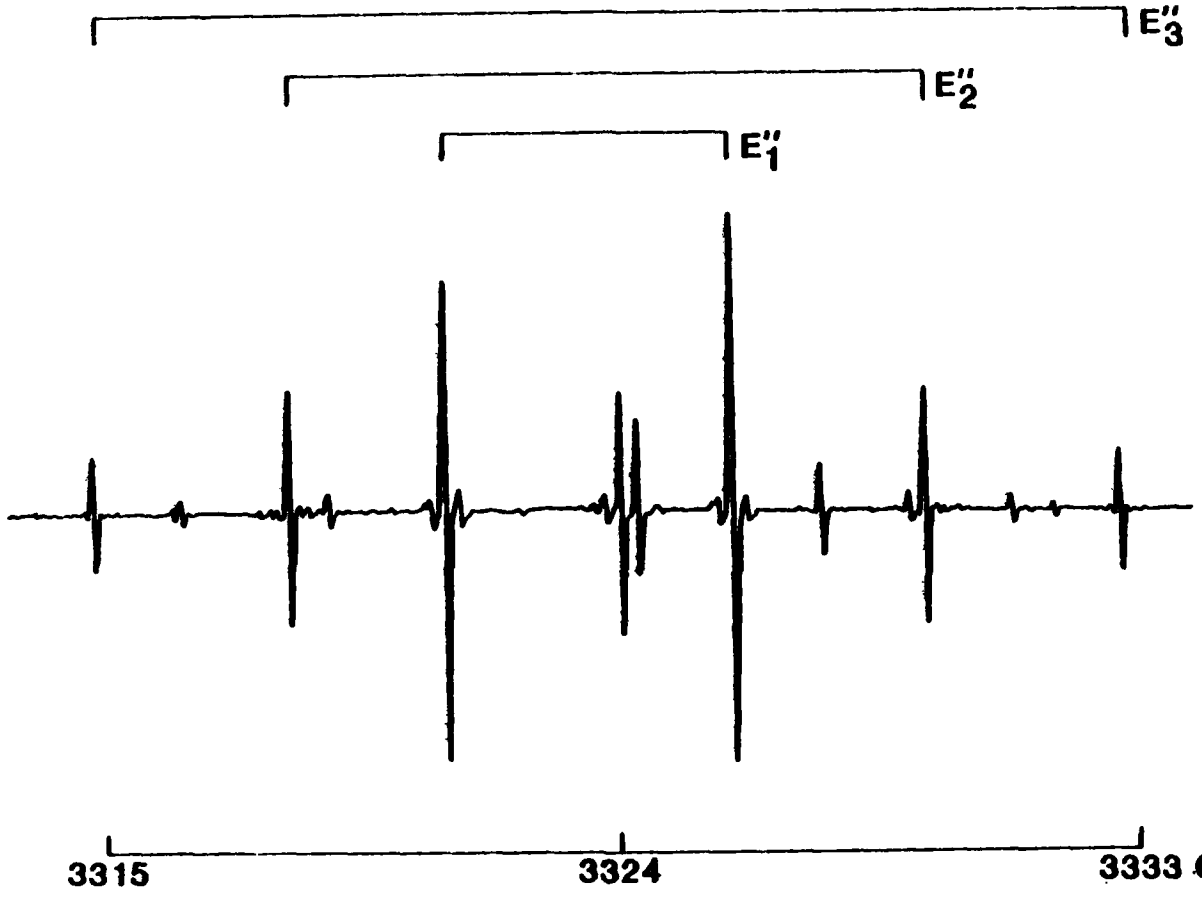

Figure 16. ESR spectrum of the E_1'', E_2'', and E_3'' centers in unswept α-quartz. The magnetic field is parallel to the c axis of the crystal and the microwave frequency is 9.3092 GHz. Many of the smaller lines are unidentified.

hyperfine lines having splittings of less than a gauss. Not shown in Fig. 16 but also observed to be centered on each E" primary doublet are eight hyperfine lines, four at higher magnetic field and four at lower magnetic field, due to strong hyperfine interactions with two slightly inequivalent ^{29}Si nuclei. These latter hyperfine splittings are approximately 200 gauss and, thus, are about one-half of the equivalent ^{29}Si hyperfine splitting for the E_1' center. Table V lists the c-axis magnetic field positions of the primary doublet and eight strong ^{29}Si hyperfine lines for each of the three E" centers. The g_c values obtained from the primary doublets are 2.0012, 2.0010, 2.0020 for the E_1'', E_2'', and E_3'' centers, respectively. As the magnetic field is rotated in the plane perpendicular to the X axis of the crystal (i.e., the crystallographic $\vec{a}_1$ axis), each of the c-axis doublets is observed to split into three less-intense doublets. The doublet separations change significantly with angle whereas the center field for each of the doublets depends only slightly on angle. The maximum primary doublet separation approaches 192 gauss for the E_1 center, 64 gauss for the E_2 center, and 51 gauss for the E_3 center. Such a large angular dependence of the doublet separations suggests that these centers are S = 1 spin systems. The other alternative would be S = 1/2, I = 1/2 (100% abundant) spin systems, but our observation of the "half-field" $\Delta M_s = \pm 2$ transitions has eliminated this latter possibility and confirmed the S = 1 nature of the E" centers.

An isochronal pulse-anneal of the three E" centers was performed in the temperature range from 8°C to 100°C. The ESR spectra were recorded at 8°C after a five minute anneal at each elevated temperature. The results, given in Fig. 17 show that the E_2'' centers anneal near 50°C while the E_1'' and E_3'' centers are more stable and anneal near 85°C and 95°C, respectively. If a sample containing E" centers is maintained at room temperature, the E_2 centers anneal out in a few hours while the E_1'' and E_3'' centers anneal more slowly and

TABLE V The c-axis magnetic field positions of the primary doublet and the eight ^{29}Si hyperfine lines for each of the three E'' centers. The magnetic field values are in Gauss and the microwave frequency is 9.3165 GHZ

	Primary Lines	Low Field Hyperfine Lines	High Field Hyperfine Lines
E_1''	3323.74	3219.43	3414.75
	3328.75	3223.18	3427.54
		3224.25	3427.54
		3227.44	3430.75
E_2''	3321.08	3191.50	3377.84
	3332.10	3212.25	3383.99
		3218.21	3427.08
		3235.13	3444.43
E_3''	3317.59	3167.22	3392.02
	3335.47	3191.85	3401.66
		3243.72	3444.43
		3253.48	3465.68

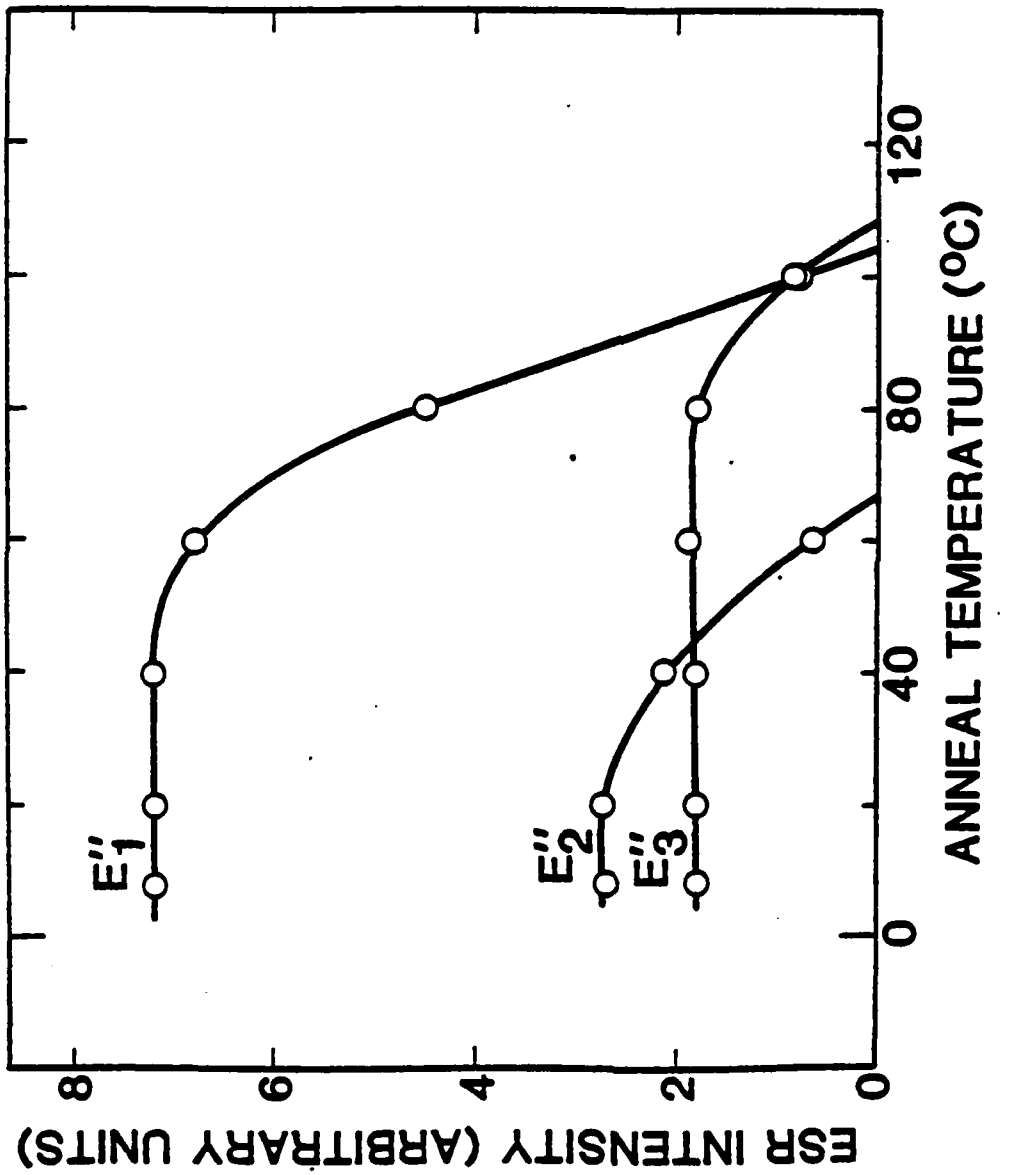

Figure 17. Thermal stability of the E'' centers as determined by five minute pulse anneals at progressively higher temperatures. The monitoring temperature was 8°C.

are gone only after several days. After being destroyed by thermal annealing (below 120°C), the E'' centers can be brought back to their initial concentrations by a short irradiation at 77 K.

The production of E'' centers in quartz is strongly dependent on previous sample treatment. As described earlier, irradiation at 77 K of an as-grown sample produces very few E'' centers, whereas irradiating the same sample at room temperature and then irradiating at 77 K causes nearly a factor of 100 increase in the E'' center concentration. This indicates that the production of the E'' centers is a two-step process, i.e., the initial room-temperature irradiation changes "precursor" defects into intermediate configurations which are then converted into E'' centers by the subsequent 77 K irradiation.

The growth of the E_1'' center concentration with room-temperature irradiation is illustrated in Fig. 18. Similar results are found for the E_2'' and E_3'' centers. Each room-temperature irradiation in this study was followed by a short two-minute irradiation at 77 K. This latter irradiation was necessary to convert into E'' centers all the intermediate configurations formed by the room-temperature irradiation. The approximate room temperature dose on the sample after 20 minutes of irradiation time is 2×10^{15} electrons/cm^2. The slow growth with room-temperature irradiation indicates that the process which transforms the "precursor" defect may involve the displacement of ions within the lattice. Interstitial protons (H^+) and alkalis (Li^+ and Na^+) known to be present in all quartz as charge compensators are possible candidates for the ions being moved by the room-temperature irradiation.

A variable-temperature irradiation study of an as-grown quartz sample was performed where each irradiation at an intermediate temperature was followed by a short 77 K irradiation (again to populate all potential E'' centers). The

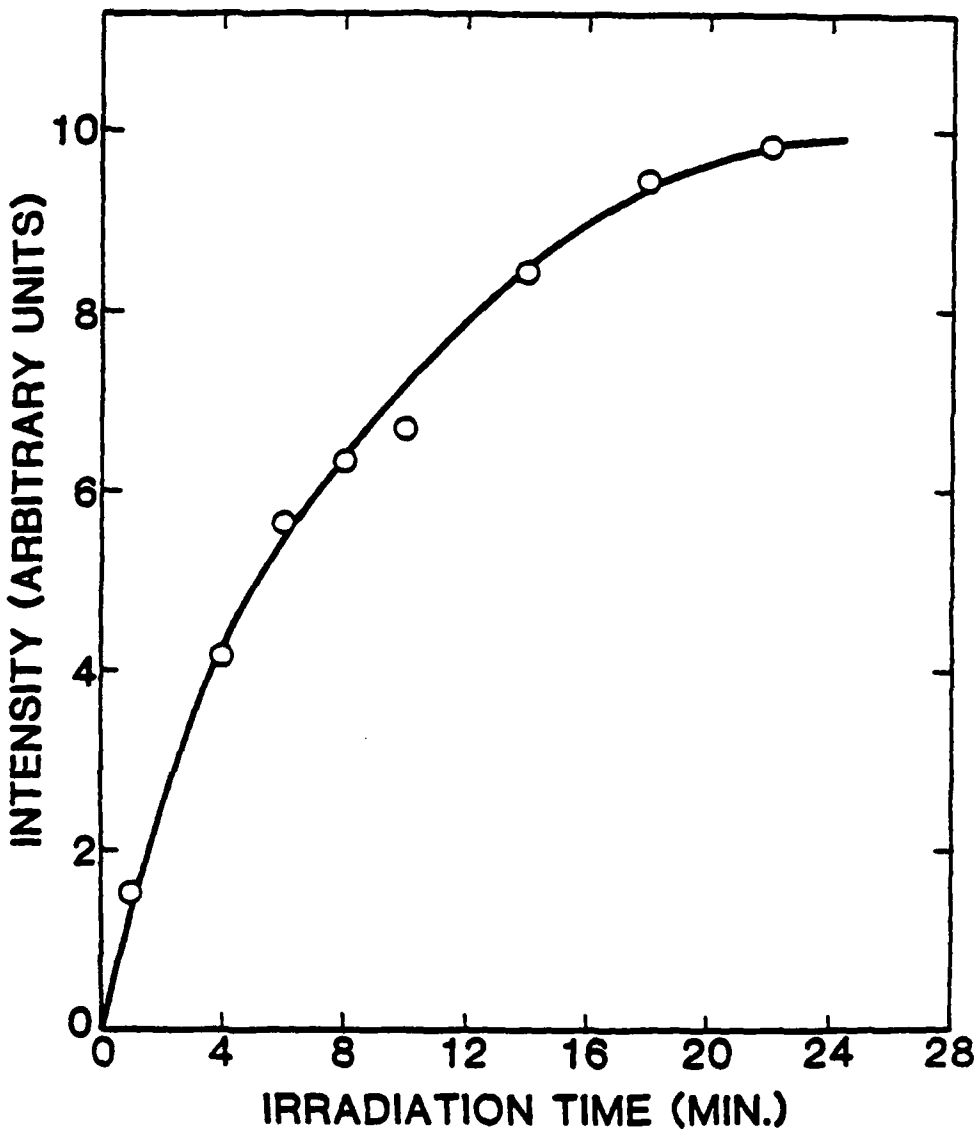

Figure 18. Growth of the E_1'' center with room-temperature irradiation. Each data point represents the total concentration corresponding to that accumulated radiation dose. A two-minute irradiatio at 77 K followed each additional room-temperature irradiation.

results, plotted in Fig. 19, show that a 77 K irradiation will not produce the E'' centers unless the sample has been previously irradiated above 200 K.

Although the magnetic resonance signals for all of the E'' centers disappeared after a thermal anneal at 120°C, they could be re-created by a short 77 K irradition. This indicates that the anneal has converted the centers to an unidentified non-paramagnetic form, but not back to the initial "precursor" defect. If they had returned to the initial "precursor" form as a result of the anneal to 120°C, a room temperature irradiation would be required before the 77 K irradiation in order to re-create the E'' centers. A series of thermal anneals above 120°C was performed on a quartz sample containing E'' centers to determine at what temperature the initial "precursor" defect is restored so that the E'' centers can not be re-created by just a 77 K irradiation. The results of this high-temperature-anneal sequence are shown in Fig. 20, where each anneal lasted 15 minutes and was followed by a short 77 K irradiation. After the anneal at 600 K, the number of E_1'' centers formed by the 77 K irradiation is seen to decrease. An anneal above 750 K converts all the E'' centers back into their "precursor" form and returns the quartz sample to its as-grown state.

The E'' centers have been produced in all unswept quartz samples at our disposal, and the most intense ESR spectra were observed in samples with the highest concentration of aluminum impurities, as detected by the presence of $[Al_e^+]^\circ$ centers. On the other hand, the E'' centers could be produced only in very small numbers in quartz samples that had been completely swept in an air or hydrogen atmosphere. Such sweeping removes all of the alkali interstitial ions and replaces them with protons.

D. Discussion

In previous studies of point defects in α-quartz, the radiation-induced mobility of interstitial alkali ions (Li^+ and Na^+) has proved to be of

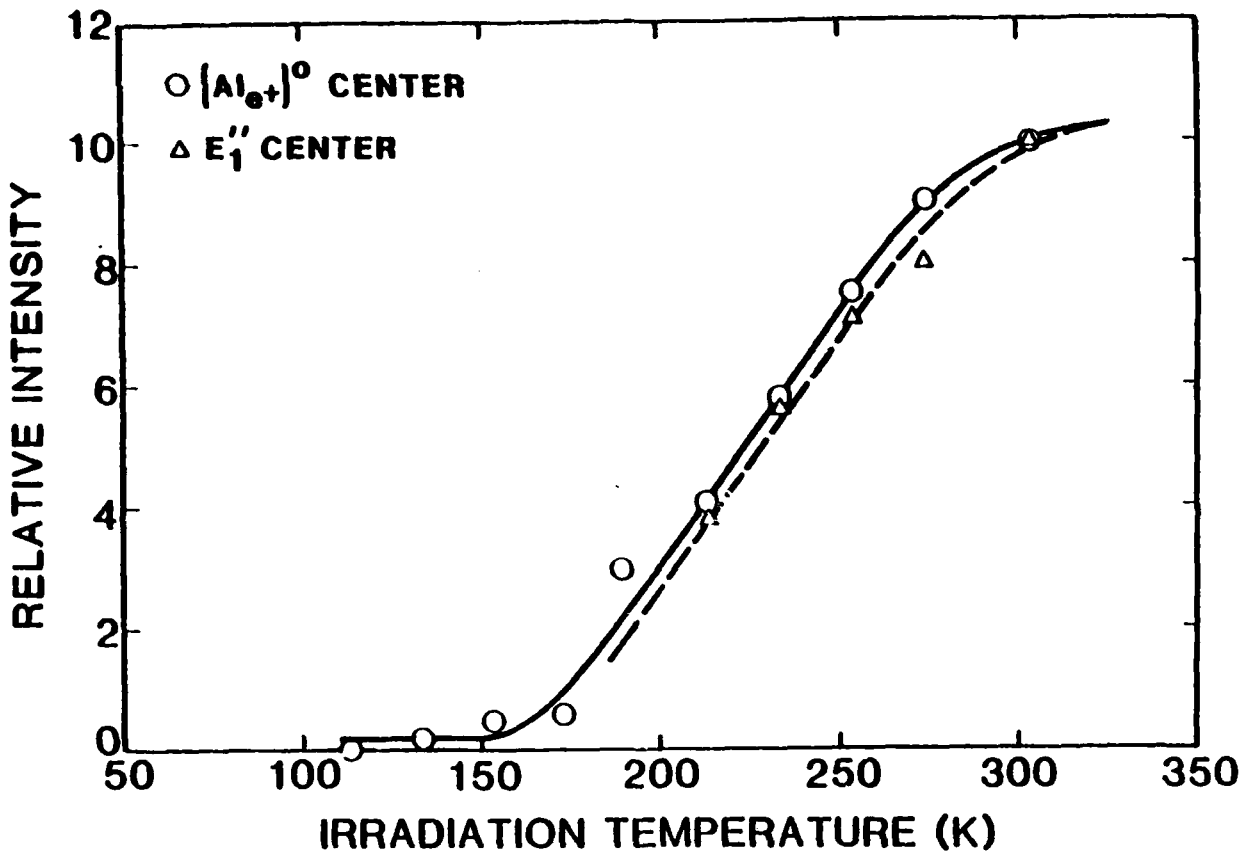

Figure 19. Production of E_1'' and $[Al_{e+}]^o$ centers as a function of the intermediate irradiation temperature. Similar results are found for the E_2 and E_3 centers.

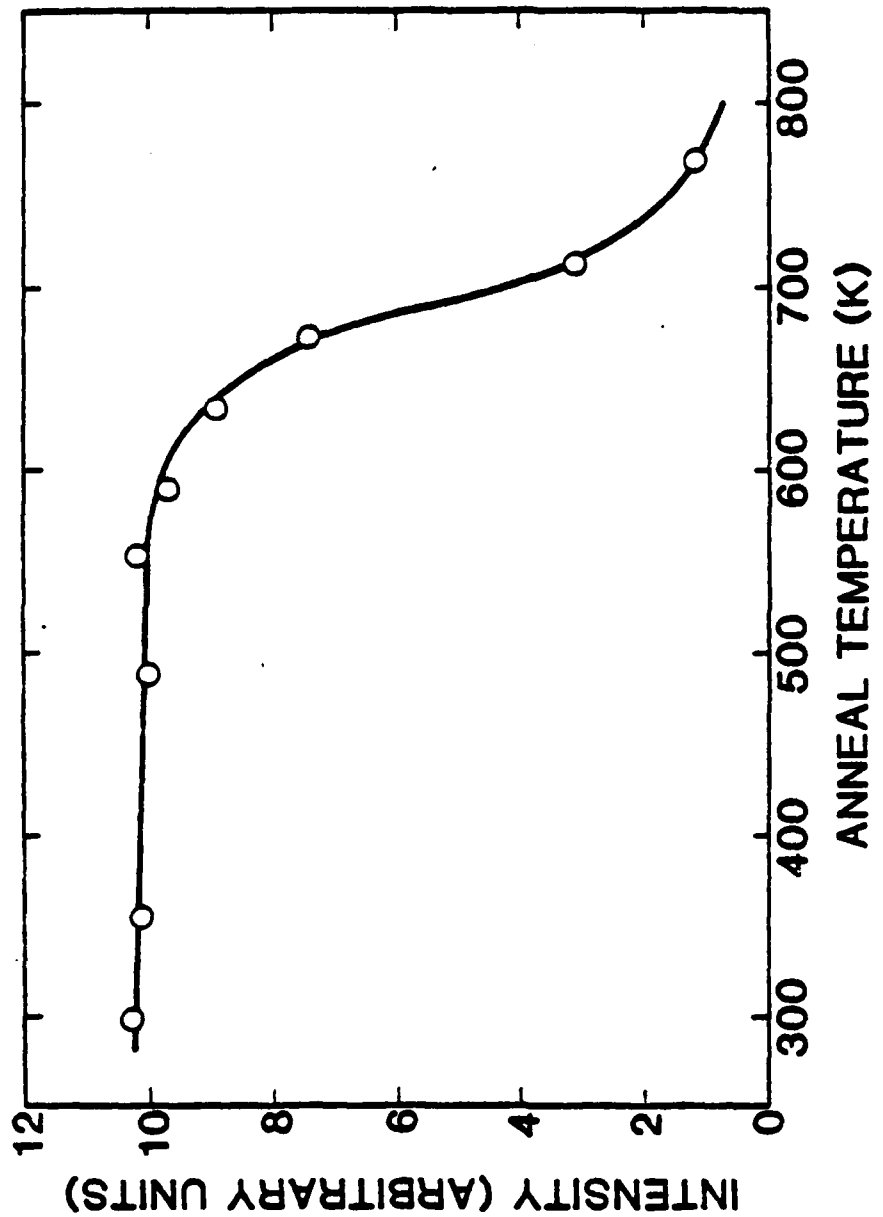

Figure 20. Concentration of F_1'' centers created by a 77 K irradiation after annealing to each given temperature for 15 minutes.

fundamental importance. These interstitials are present in all as-grown quartz and are initially located adjacent to the ubiquitous Al^{3+} substitutional ions, where they act as charge compensators. In ESR studies, Markes and Halliburton[7] have shown that the interstitial alkali ions become mobile under irradiation at temperatures above 200 K (see also data in Fig. 19). Acoustic loss measurements by Doherty et al.[8] also support this result. Once the interstitial alkali ions are released by the radiation, they diffuse along the c-axis channels and become stably trapped at unidentified sites within the crystal. Heating above 750 K frees the interstitial alkalis from these traps and allows them to return to the Al^{3+} sites, thus restoring the crystal to its as-grown condition.

Many similarities are found when comparing the production and thermal annealing characteristics of the E'' centers, which are described in the present section, with the previously reported [5,7] behavior of the interstitial alkali ions. The most important observation is that E'' centers are found in large concentrations only in unswept quartz or in partially swept quartz; i.e., E'' centers are only produced when interstitial alkali ions are present in the crystal. Also, E'' centers can not be created in an as-grown sample unless it has been irradiated above 200 K; similarly, interstitial alkali ions can not be removed from Al^{3+} sites unless the irradiation temperature is above 200 K. Annealing a previously-irradiated sample above 750 K restores the precursor state of the E'' center, and the same anneal returns the interstitial alkali ions to the Al^{3+} sites.

These results indicate that movement of the interstitial alkali ions away from the Al^{3+} sites (by radiation at suitable temperatures) accompanies the production of the E'' centers. There is, however, no evidence that the alkali ions are a direct part of the E'' centers. Both lithium and sodium have a

high-abundance isotope (^{7}Li and ^{23}Na) with nuclear spin of 3/2. Since the ESR linewidths of the E'' centers are extremely narrow (less than 0.05 gauss), a hyperfine interaction with either of these two nuclei would result in observable splittings in the ESR spectra if the alkali ion were near the unpaired electron spin system. No such splittings are found in the ESR spectra of the E'' centers.

Until complete sets of spin-Hamiltonian parameters are determined for the E'' centers, specific models can not be developed. However, some general properties the models will undoubtedly possess can be outlined. The narrow ESR linewidths, long spin-lattice-relaxaton times, and small negative g shifts indicate that the E'' centers must involve electrons associated with oxygen vacancies, in direct analogy to the E_1', E_2', and E_4' centers in quartz. The S = 1 nature of the E'' centers suggests a model involving two nearby oxygen vacancies, each with a single unpaired electron. To a first approximation, this would be equivalent to two neighboring E_1' centers. This view is supported by the two slightly inequivalent strong ^{29}Si hyperfine interactions observed for each E'' center. Using the maximum fine-structure splitting of the E_1 center (195) gauss), and assuming a dipole-dipole interaction, the separation of the two electrons can be estmated. The separation value arrived at by this procedure is approximately 5 Å for the E_1'' center and is even larger for the other two centers.

VI. EVALUATION OF RADC-GROWN QUARTZ

Several years ago the Air Force established the Hydrothermal Growth Facility at RADC, Hanscom AFB. As part of our contract we performed several evaluation tests on the Air Force grown material. Aluminum is a pervasive and active impurity in quartz. We are using the ESR test developed by Markes and Halliburton[7] to measure the aluminum content in RADC-grown quartz. Table VI

TABLE VI SUMMARY OF ALUMINUM ANALYSIS

OF RADC-GROWN QUARTZ

SAMPLE	Al content (ppm)
X7-1 (X growth)	21.0
X7-1 (Z growth)	4.6
X7-2 (Z growth)	11.0
X7-3 (Z growth)	4.6
X7-4 (Z growth)	9.0
X23 (seed)	2.0
X23	~967.0
X33	7.1
F2	12.4
QA4-P (Boule 1)	16.4
QA4-U (Boule 2)	19.8
QA5-B	0.9
QA6	0.8
QA7	1.7
QA8-B	0.9
QA8-T	0.7
QA9 (Large Boule)	9.4
QA9 (Small Boule)	1.3
QA10 (Large Boule)	1.8
QA10 (Small Boule)	3.5

*Aluminum content measured by the electron spin resonance (ESR) technique, as described by Markes and Halliburton [J. Appl. Phys. 50, 8172 (1979)]. All measurements were performed at Oklahoma State University.

presents the results of this investigation.

"As-grown" synthetic alpha-quartz also contains OH-related defects, which cause infrared bands at 3585cm^{-1}, 3437cm^{-1}, and 3400cm^{-1}, as shown in Fig. 21. Dodd and Fraser[53] and later Sawyer[54] have shown that the mechanical Q of a crystal is related to the OH content of the quartz. This result has led to the routine use of room temperature infrared absorption as a method of predicting the Q of a quartz stone. This optical Q is usually determined by measuring the room temperature absorption coefficient at 3500cm^{-1}. Basically, this measurement picks up the temperature broadened 3437cm^{-1} and 3400cm^{-1} OH bands. Early internal friction studies by Jones and Brown[55] showed that both the Na loss peak and the room temperature acoustic loss of 5 MHz 5th overtone AT-cut crystals increased with the rate at which the original stone was grown. As a joint project with Dr. A. F. Armington of RADC we are investigating the relation between the strength of these OH^- related absorption bands and the crystal growth rate.

Pure Z-growth Z-plates were prepared for this study from stones grown at the Air Force Hydrothermal Facility. The growth rate for quartz is defined as the increase in thickness of the stone, including both sides, per unit time in the direction perpendicular to the seed plate. All infrared absorption measurements were taken with the sample at liquid nitrogen temperature. In order to check for the presence of aluminum, a second absorption scan was made after the sample was irradiated at room temperature. A room temperature irradiation converts the Al-alkali center which is present in as-grown quartz into Al-OH^- and Al-hole centers. The Al-OH^- center is responsible for the 3367cm^{-1} and 3306cm^{-1} bands. Fig. 21 shows a typical absorption spectrum for a sample grown at a relatively fast rate. Figure 22 shows the absorption coefficients of the 3585cm^{-1} and the 3400cm^{-1} bands as a function of growth

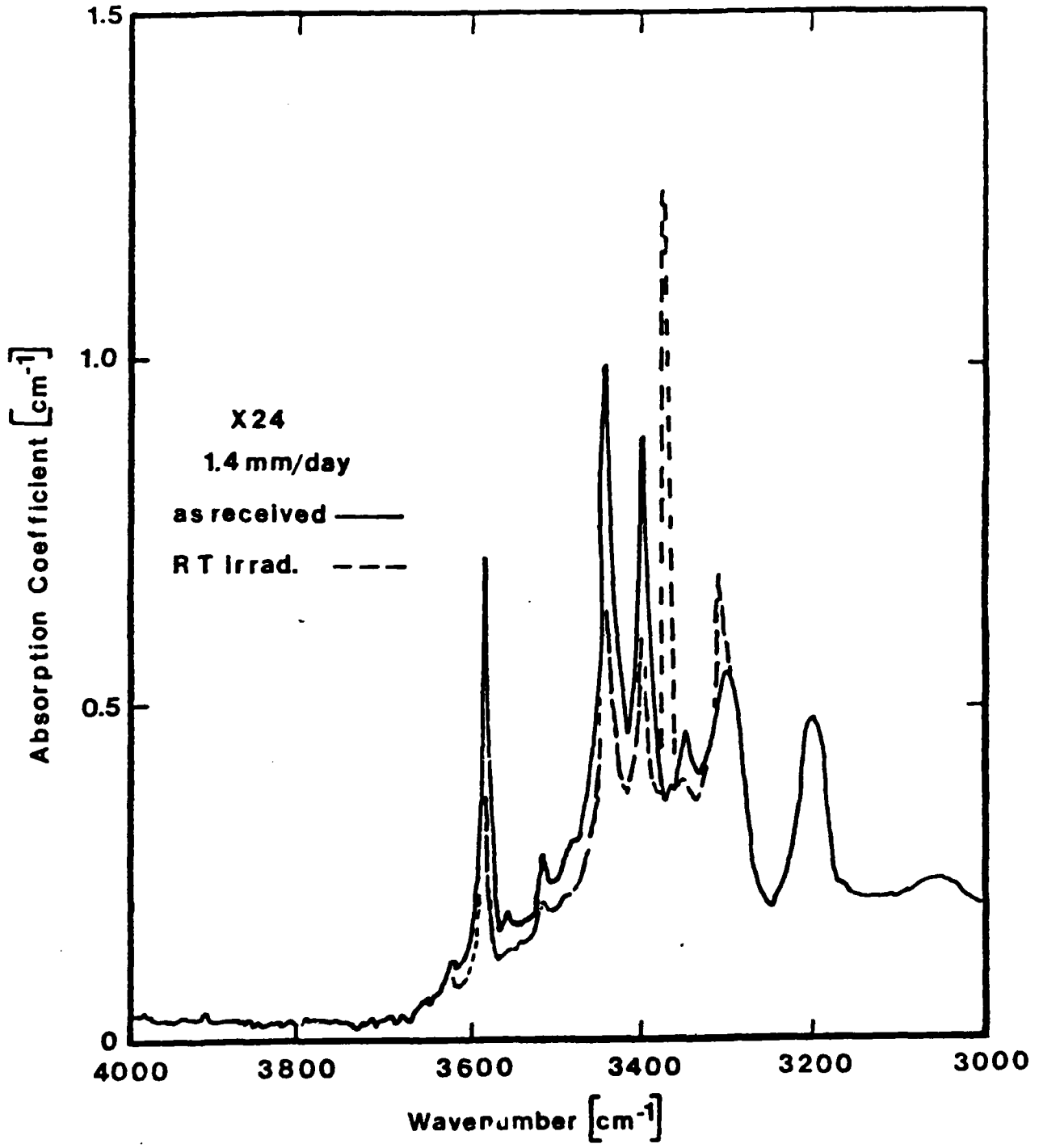

Figure 21. The solid curve shows the infrared absorption spectrum for a fast-growth sample. The 3585, 3437, and 3400 cm^{-1} OH^- bands are large. The dashed curve shows that a room-temperature irradiation reduces these OH^- bands and produces the 3367 and 3306 cm^{-1} Al-OH^- bands.

rate. Both bands increase in essentially the same manner. Figure 23 shows that the 3437cm^{-1} band also increases at the same rate as the 3585cm^{-1} band. All three bands are due to OH^- related defects since when the sample is swept in a D_2 atmosphere as described earlier in this report they are replaced by their OD analogs.[56] However, the proton trap or traps are unknown.

When quartz is irradiated at room temperature the interstitial alkali ions at the aluminum site are replaced by either protons or holes on a non-bonding orbital of an adjacent oxygen. The protons come from the OH^-related defects described above. To a good approximation the resulting decreases in the 3585, 3437, and 3400cm^{-1} bands acounts for the size of the 3367 and 3306cm^{-1} Al-OH^-bands.[6] Since the Al-hole center is also produced by a room temperature irradiation the height of the 3367 and 3306cm^{-1} bands does not give the total aluminum content. However, their presence does indicate the relative aluminum concentration. Figure 24 shows the 3367cm Al-$OH^-$and 3585cm^{-1} OH band absorption coefficients versus growth rate. The Al-OH^-band increases somewhat faster than the 3585cm^{-1} band. The heights of the 3367 and 3306cm^{-1} bands in the samples grown at 1.27 mm/day and 0.3 nm/day indicate approximately 6 and 0.5 ppm Al-OH^-centers, respectively. The ESR test for aluminum was performed and showed 12.4 and 0.9 ppm Al, respectively, for the two samples.

The defects responsible for the OH^- related bands at 3585, 3437, and 3400 cm^{-1} increase rapidly for crystal growth rates greater than 0.7 mm/day. All three bands grow together. The aluminum content also increases with growth rate.

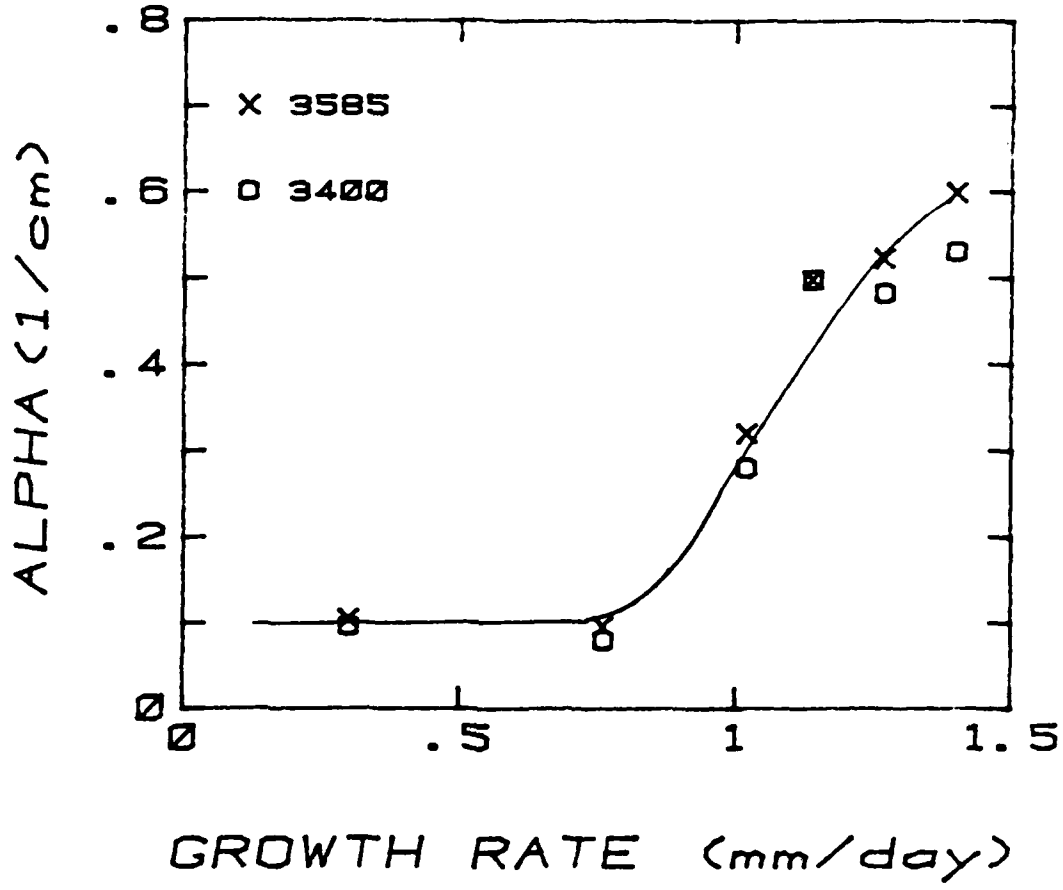

Figure 22. The height of the 3585 and 3400 cm^{-1} OH^- -related bands shown as a function of growth rate.

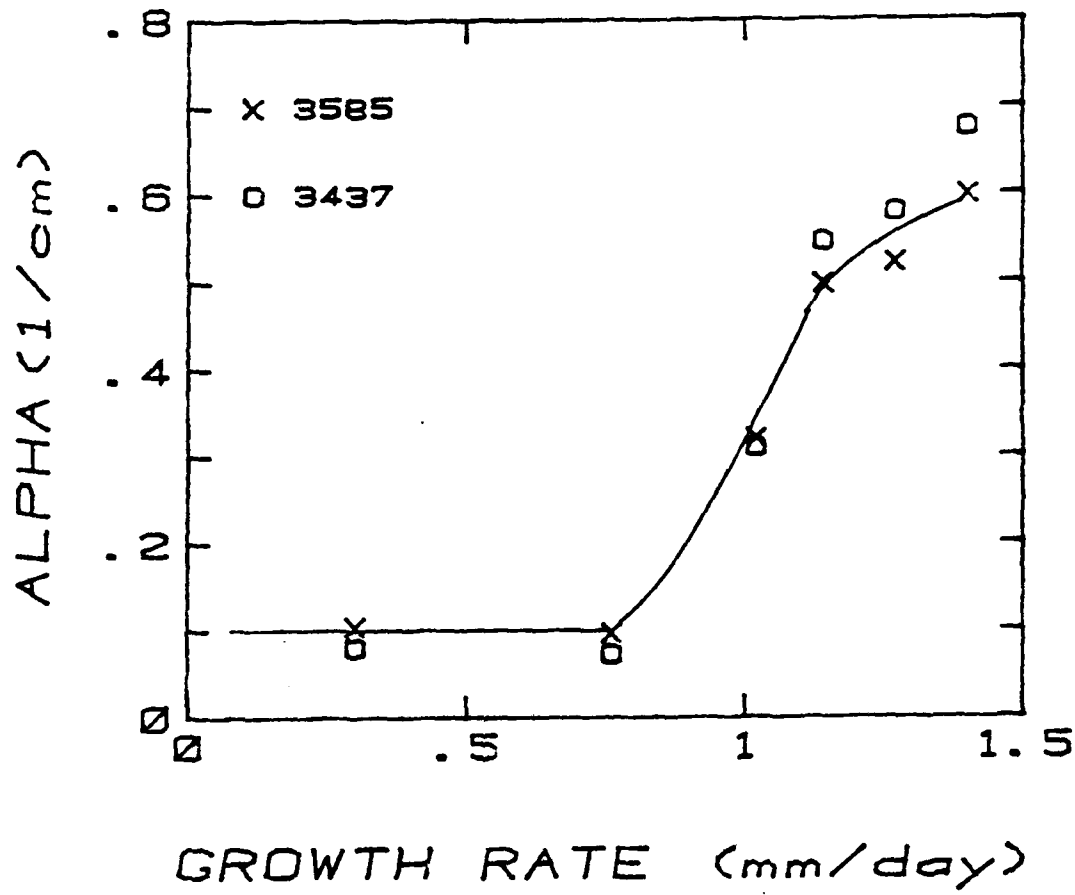

Figure 23. The heights of the 3585 and 3437 cm^{-1} OH^- -related bands are shown as a function of growth rate.

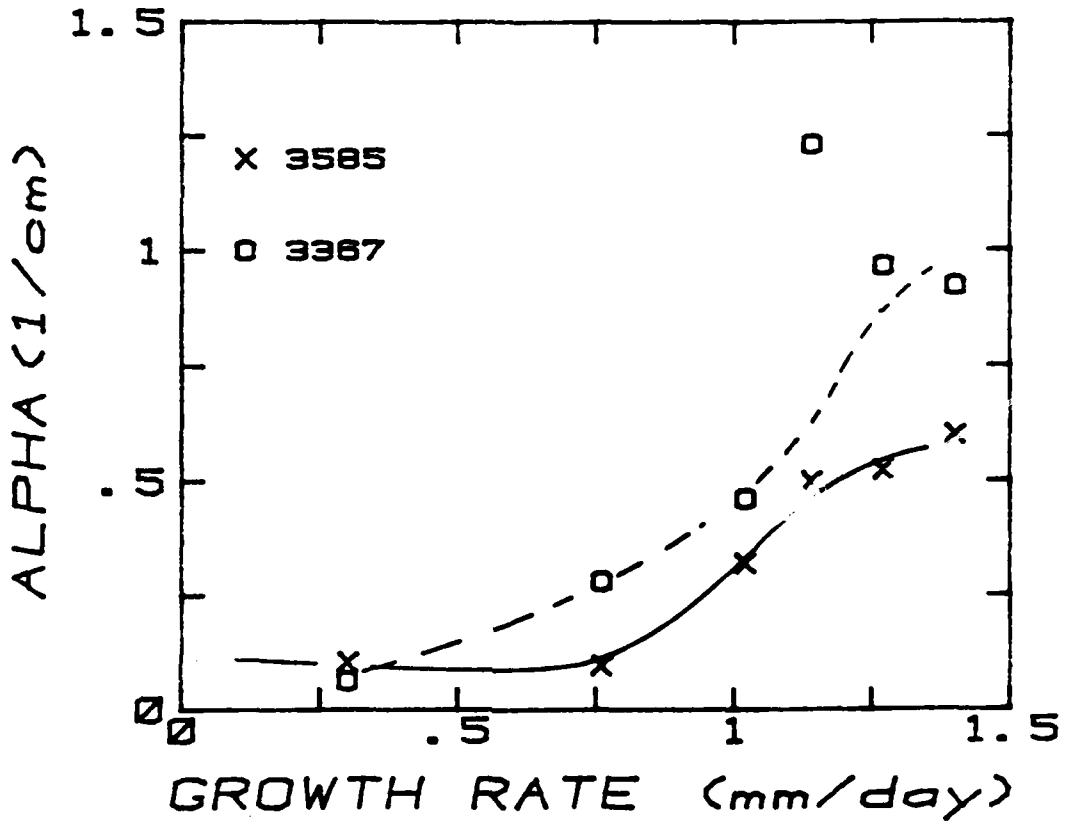

Figure 24. The 3585 OH^- defect band and the 3367 cm^{-1} Al-OH^- band are shown as a function of the growth rate.

VII. REFERENCES

1. D. B. Fraser, Physical Acoustics, (Ed. W. P. Mason), Vol. 5, Chapter 2, Academic Press, New York, 1968.

2. T. M. Flanagan and T. F. Wrobel, IEEE Trans. Nucl. Sci. NS-16, 130 (December, 1969).

3. B. R. Capone, A. Kahan, R. N. Brown, and J. R. Buckmelter, IEEE Trans. Nucl. Sci. NS-17, 216 (December, 1970).

4. J. C. King and H. H. Sander, IEEE Trans. Nucl. Sic. NS-19, 23 (1972).

5. L. E. Halliburton, N. Koumvakalis, M. E. Markes, and J. J. Martin, J. Appl. Phys. 52, 3565 (1981).

6. W. A. Sibley, J. J. Martin, M. C. Wintersgill and J. D. Brown, J. Appl. Phys. 50, 5449 (1979).

7. M. E. Markes and L. E. Halliburton, J. Appl. Phys. 50, 8172 (1979).

8. S. P. Doherty, J. J. Martin, A. F. Armington, and R. N. Brown, J. Appl. Phys. 51, 4104 (1980).

9. J. C. King, Bell System. Tech. J. 38, 573 (1959).

10. A. Kats, Phillips Res. Rep. 17, 133 (1962).

11. D. B. Fraser, J. Appl. Phys. 35, 2913 (1964).

12. Gerdu B. Kreft, Rad. Effects. 26, 249 (1975).

13. R. N. Brown, J. J. O'Conner, and A. F. Armington, Mat. Res. Bull. 15, 1063 (1980).

14. R. A. Poll and S. L. Ridgway, IEEE Trans. Nuc. Sci. NS-13, 130 (1966).

15. P. Pellegrini, F. Euler, A. Kahan, T. M. Flanagan and T. F. Wrobel, IEEE Trans Nuc. Sci., NS-25, 1267 (1978).

16. H. Jain and A. S. Nowick, J. Appl. Phys. 53, 477 (1982).

17. P. Pellegrini, F. Fuler, A. Kahan, T. M. Flanagan, and T. F. Wrobel, IEEE Trans. Nucl. Sci. NS-25, 1267 (1978).

18. T. J. Young, D. R. Koehler, and R. A. Adams, Proceedings of the 32nd Annual Symposium on Frequency Control, 34 (1978).

19. T. M. Flanagan, IEEE Trans. Nucl. Sci. NS-21, 390 (December, 1974).

20. J. J. Martin and S. P. Doherty, Proceedings of the 34th Annual Symposium on Frequency Control. U.S. Army Electronics Command, Fort Monmouth, NJ, pp. 81-84 (1980).

21. A. W. Warner, Bell System Technical J. 40, 1193 (1960).

22. J. C. King, A. A. Ballman and R. A. Laudise, J. Phys. Chem. Solids. 23, 1019 (1962).

23. D. S. Park and A. S. Nowick, Phys. Stat. Sol (a) 26, 617 (1979).

24. H. G. Lipson, A. Kahan, R. N. Brown and F. Euler, Proceedings of the 35th Annual Symposium on Frequency Control, U.S. Army Electronics Command, Fort Monmouth, NJ pp. 329-334 (1981).

25. D. R. Koehler. Proceedings of the 35th Annual Symposium on Frequency Control, U.S. Army Electronics Command, Fort Monmouth, NJ pp 327-328 (1981).

26. J. J. Martin, L. E. Halliburton, and R. B. Bossoli, Proceedings of the 35th Annual Symposium on Frequency Control, U.S. Army Electronics Command, Fort Monmouth, NJ pp 317-320 (1981).

27. J. M. Stevels and J. Volger, Philips Res. Repts. 17, 284 (1962).

28. A. L. Taylor and G. W. Farnell, Can. J. Phys. 42, 595 (1964).

29. J. C. King and H. H. Sander, Radiat. Eff. 26, 203 (1975).

30. J. A. Weil, Radiat. Eff. 26 261 (1975).

31. P. L. Mattern, K. Lengweiler, and P. W. Levy, Radiat. Eff. 26, 237 (1975).

32. G. H. Sigel, J. Non-Cryst. Solids 13, 372 (1973/74).

33. D. L. Griscom, Proceedings of the Thirty-Third Annual Symposium on Frequency Control, 98 (1979).

34. A. N. Trukhin and A. E. Plaudis, Sov. Phys. Solid State 21, 644 (1979).

35. B. P. Gritsenko, V. M. Lisitsyn, and V. N. Stepanchuk, Sov. Phys. Solid State 23, 222 (1981).

36. E. J. Friebele, D. L. Griscom, M. Stapelbroek, and R. A. Weeks, Phys. Rev. Lett. 42, 1346 (1979).

37. D. M. Malik, E. E. Kohnke, and W. A. Sibley, J. Appl. Phys. 52, 3600 (1981).

38. J. H. Mackey, J. Chem. Phys. 39, 74 (1963).

39. R. A. Weeks, J. Appl. Phys. 27, 1376 (1956).

40. R. H. Silsbee, J. Appl. Phys. 32, 1459 (1961).

41. F. J. Feigl, W. B. Fowler, and K. L. Yip, Solid State Commun. 14, 225 (1974).

42. K. L. yip and W. B. Fowler, Phys. Rev. B 11, 2327 (1975).

43. R. A. Weeks and C. M. Nelson, J. Am. Ceram. Soc. 43, 399 (1960).

44. R. A. Weeks, Phys. Rev. 130, 570 (1963).

45. J. G. Castle, D. W. Feldman, P. G. Klemens, and R. A. Weeks, Phys. Rev. 130, 577 (1963).

46. L. E. Halliburton, B. D. Perlson, R. A. Weeks, J. A. Weil, and M. C. Wintersgill, Solid State Commun. 30, 575 (1979).

47. B. M. Moiseev, P. O. Okulevich, and L. T. Rakov, Sov. Phys. Crystallogr. 25, 370 (1980). Translated from Kristollografiya 25, 640 (1980).

48. J. Isoya, J. A. Weil, and L. E. Halliburton, J. Chem. Phys. 74, 5436 (1981).

49. Weeks and Nelson, in reference 43, have previously used the E'' notation to refer to an oxygen vacancy that contains two electrons in an S = 0 configuration.

50. R. A. Weeks and M. M. Abraham, Solid State Division Annual Progress Report, Oak Ridge National Laboratory, USA, p. 36 (1964).

51. R. A. Weeks and M. M. Abraham, Bull; Am. Phys. Soc. 10, 374 (1965).

52. V. P. Solntsev, R. I. Mashkovtsev, and M. Ya. Shcherbakova, J. Struct, Chem. 18, 578 (1977). Translated from Zhurnal Strukturnoi Khimii, 18, 729 (1977).

53. D. M. Dodd and D. B. Fraser, J. Phys. Chem. Solids. 26, 673 (1965).

54. B. Sawyer, IEEE Trans. Sonics and Utrasonics, SU-19, 411 (1972).

55. C. K. Jones and C. S. Brown, Proc. Phys. Soc. 79, 930 (1962).

56. Nicholas Koumvakalis and Mark Markes, J. Appl. Phys. 51, 3431 (1980).

MISSION
of
Rome Air Development Center

RADC plans and executes research, development, test and selected acquisition programs in support of Command, Control Communications and Intelligence (C^3I) activities. Technical and engineering support within areas of technical competence is provided to ESD Program Offices (POs) and other ESD elements. The principal technical mission areas are communications, electromagnetic guidance and control, surveillance of ground and aerospace objects, intelligence data collection and handling, information system technology, ionospheric propagation, solid state sciences, microwave physics and electronic reliability, maintainability and compatibility.

Printed by
United States Air Force
Hanscom AFB, Mass. 01731

END

FILMED